U.S. DEPARTMENT OF
ENERGY

Office of
ENERGY EFFICIENCY &
RENEWABLE ENERGY

Dim-to-Warm LED Lighting: Stress Testing Results for Select Products

U.S. Department of Energy—Solid-State Lighting Technology Area

January 2020

(This page intentionally left blank)

RTI Project Number
0215939.001.001

Dim-to-Warm LED Lighting: Stress Testing Results for Select Dim-to-Warm Products

January 2020

Prepared for

U.S. Department of Energy

Through contract with
KeyLogic Systems, Inc.
3168 Collins Ferry Road
Morgantown, WV 26505

Prepared by

Kelley Rountree, Lynn Davis, Michelle McCombs, Roger Pope, Jean Kim, and Karmann Mills
RTI International
3040 E. Cornwallis Road
Research Triangle Park, NC 27709

Monica Hansen
LED Lighting Advisors
3047 Marilyn Way
Santa Barbara, CA 93105

Acknowledgments

This material is based upon work supported by the U.S. Department of Energy, Office of Energy Efficiency and Renewable Energy (EERE), under Award Number DE-FE0025912.

This work benefited greatly from input and discussions from members of the LED Systems Reliability Consortium: Morgan Pattison of SSLS, Inc, Jim Gaines of Signify, Steve Paolini of Telelumen, Wouter Soer of Lumileds, and Mark Duffy of Current by GE.

Disclaimer

Nomenclature or List of Acronyms

45OL	operational life test conducted at 45°C
6590	life test conducted at 65°C and 90% relative humidity
α	decay rate constant in TM-28-14 model
$\Delta u'$	change in the *u'* coordinate of chromaticity
$\Delta u'v'$	chromaticity shift or the total change in chromaticity coordinates
$\Delta v'$	change in the *v'* coordinate of chromaticity
λ_c	centroid wavelength
A	amperes or amps
ac	alternating current
ANSI	American National Standards Institute
AST	accelerated stress test
CCT	correlated color temperature
CIE	International Commission on Illumination
COB	chip-on-board
CRI	color rendering index
CSM	chromaticity shift mode
CSP	chip-scale package
D2W	dim-to-warm
dc	direct current
DUT	device under test
hrs	hours
Hz	Hertz or cycles per second
IEEE	Institute of Electrical and Electronics Engineers
IES	Illuminating Engineering Society
IC	integrated circuit
K	Kelvin
L70	time required for the luminous flux to decay to 70% of the initial value
LED	light-emitting diode

LFM	luminous flux maintenance
lm	lumen
LSRC	LED Systems Reliability Consortium
MP-LED	mid-power LED
NEMA	National Electronics Manufacturing Association
NIST	National Institute of Standards and Technology
NGLIA	Next Generation Lighting Industry Alliance
nm	nanometer
P_{st}	short-term flicker indicator
PCB	printed circuit board
R_f	fidelity index in IES TM-30-18
R_g	gamut index in IES TM-30-18
RTOL	room temperature operational life
SPD	spectral power distribution
SSL	solid-state lighting
SVM	stroboscopic visibility measure
t	time
T_{95}	time required to reach 95% of equilibrium temperature
TLA	temporal light artifact
u'	chromaticity coordinate in the CIE 1976 color space
V	volt
v'	chromaticity coordinate in the CIE 1976 color space
W	watt
WTL	white-tunable lighting
W/nm	watts per nanometer

Executive Summary

Solid-state lighting (SSL) products that use light-emitting diodes (LEDs) offer numerous advantages over conventional lighting products including energy savings, longer lifetimes, and greater spectral flexibility of the output light from the device. Dim-to-warm (D2W) products are an emerging SSL technology for use in residential and entertainment applications. D2W products are a type of multi-source LED product and a subclass of white-tunable lighting (WTL) that mimic the behavior of incandescent lamps as they are dimmed; D2W products provide a warmer lighting spectrum (i.e., the correlated color temperature [CCT] shifts to a lower value) as the user dims the device. Since the CCT of LEDs does not change drastically with dimming, new electrical architectures and circuits are needed to provide this "warm-dimming" capability in LED products. The effect of these architectures and dimming on the reliability of the D2W lamps and luminaires is not well understood. Therefore, this report, which is the second report about D2W LED lighting products, uses accelerated stress tests (AST) to study and understand the mechanisms of optical change of the D2W products. The earlier report (Initial Benchmarks) [1] on D2W products provided initial characterization of the lamps and LED modules studied in this current report. The earlier report also provided performance benchmarks relative to an incandescent lamp for the lamps studied in this current report.

The selected D2W products investigated in this report used different electrical architectures to control power to their LED primaries, and the electrical architectures could be broadly categorized into two groups (Architecture 1 and Architecture 2). At low power and deep dimming, both architectures only supplied enough power to operate the lower CCT LED primary and at moderate dimming levels, the lower CCT LED primary and at least one or more higher CCT LED primaries emit light. The electrical architectures differed at high power (e.g., no dimming), where the lower CCT LED primary turned off in Architecture 1 but the lower CCT LED primary (and all other LED primaries) remained on for Architecture 2. The specific devices under test (DUTs) examined in this report include four lamps (referred to as Lamp A – Lamp D) and three integrated LED solutions or LED modules (referred to as Module E – Module G). Lamps A, B, and D used Architecture 1 while Lamp C and Modules E – F used Architecture 2 to provide the warm-dimming behavior. In general, the DUTs examined provided spectral tuning in a warm CCT range (1,800 K – 3,000 K); Module G provided spectral tuning in a cooler CCT range (2,700 K – 4,000 K).

The four lamps were either A-style (Lamps A and B) or candelabra-style (Lamps C and D). The A-style lamps were 60-watt equivalent and the candelabras were 40-watt equivalent. Both styles were intended for indoor or outdoor use to promote the familiar warm-dimming characteristics of incandescent lamps. The LED primaries for each D2W product investigated in this report were unique to each other by way of packaging (plastic mid-power LEDs [MP-LEDs] or ceramic MP-LEDs), LED array format (chip-on-board [COB] or chip-scale package [CSP]), LED type, phosphor material, and size. Lamps A, B, and D used plastic MP-LEDs while Lamp C used ceramic MP-LEDs. Lamps A, C, and D had traditional LED lamp design, meaning that their LED packages were mounted to a central printed circuit board (PCB) on a heat sink and the lamp relied on plastic lenses and reflectors for uniform light dispersion. Lamp B used a filament-style LED arrangement with a clear, glass globe, adding to its visual likeness of an incandescent lamp. The LED modules examined in this study were composed of LED arrays in the COB (Module E) or CSP (Modules F and G) format.

This report summarizes the overall findings from up to 11,000 hrs of AST on the D2W lamp DUTs and up to 7,000 hrs of AST on the LED module DUTs. The AST procedures used in this study included room temperature operational life (RTOL) test, 45ºC operational life (45OL) test, and a wet high-temperature operational life test performed at 65ºC and 90% relative humidity (6590). During the ASTs described herein, separate populations of each lamp DUT were subjected to power cycling through a four-step process of max power (no dimming, 100% power level), low power (dimming the power level to 10% or 25%), medium power (dimming the power level to 50%), and no power (off) during RTOL, 45OL, and 6590 testing. The dwell time at each power level for the lamp DUTs was determined by the thermal characteristics of each lamp. During the ASTs for the LED modules, separate populations of each LED module DUT were subjected to power cycling

through a 4-hr loop: 1 hr at max current, 1 hr at low current, 1 hr at moderate current, and 1 hr off during RTOL, 45OL, and 6590 testing.

This report provides details regarding the causes of chromaticity and radiant flux changes and the impacts that these changes have on the ability of the DUTs to maintain their designed warm-dimming behavior. This report provides key findings on the relative impact of the form factor (i.e., lamp style, COB, CSP); LEDs, including LED chip, phosphors, and packages; secondary device optics if applicable (e.g., lenses, reflectors); and electrical architecture on the long-term reliability of the D2W products. The impacts of the new electrical architectures and system components on product reliability may be different than other multi-source LED or WTL products, and therefore new challenges to reliability engineering must be identified and characterized to understand the performance of these new lighting technologies.

The key findings from this report and the earlier report [1] include the following:

- The reliability of the LEDs for each DUT greatly impacted the long-term chromaticity and radiant flux behavior for the D2W products. It was found in this report that the stability of the LED chip was generally good, but the stabilities of the phosphors were less reliable. In particular, the lower CCT LED primaries, which had higher red phosphor concentrations, were subject to larger chromaticity shifts in the green direction (CSM-2, where CSM stands for chromaticity shift mode).
- The secondary optics of the lamps in this study were found to have major impact on the chromaticity maintenance. In particular, the enclosure of LED primaries in a glass globe under positive pressure (Lamp B DUTs) showed great chromaticity stability ($\Delta u'v' < 0.002$ at all ASTs) relative to the traditional plastic globes, likely caused by less moisture and air ingress (two major contributors to phosphor oxidation). Additionally, the lenses for Lamps A and C became discolored during AST which led to terminal chromaticity shifts in the yellow-green direction (though parametric failure did not occur).
- The form factor of the D2W products had significant impact on the reliability of the DUTs examined in this report. At the more aggressive test conditions (i.e., 6590), the candelabra-style Lamps C and D performed the worst, with projected lifetimes to luminous flux maintenance (LFM) values below 0.70 as low as 8,174 hrs (Lamp C) and abrupt failure occurring for all Lamp D DUTs. The DUTs with A-style lamp and COB or CSP LED module form factors generally exceeded the maximum allowed lifetime projections by the TM-28-14 method. The lower performance of the candelabra-style lamps is thought to be a consequence of the more stringent space limitations in these DUTs.
- Aging of the driver electronics for the lamp DUTs examined in this study did not induce large changes in power consumption, LFM, or temporal light artifacts (TLA), and no correlation between driver architecture and device performance was found. However, the driver electronics did impact the overall reliability of the lamps, with four lamp DUTs failing abruptly due to electrical failure and two lamp DUTs failing parametrically (a Lamp B DUT exhibited a LFM value below 0.70 while a Lamp C DUT underwent chromaticity maintenance failure) due to improper regulation of current to the LED primaries by the electrical driver. The parametric failures caused by logic failures are unique to D2W products, and greater emphasis on understanding the reliability of the logic circuits should be emphasized in future studies.
- The LED modules examined herein were also susceptible to logic failure modes, and intermittent or complete failure of these logic circuits produced chromaticity shifts in excess of $\Delta u'v' = 0.018$ (one Module E DUT, one Module F DUT, and two Module G DUTs). Three of these DUTs were operated at low stress test conditions (RTOL or 45OL) and the failures appeared to be caused by manufacturing flaws (e.g., solder migration) or premature component failure as opposed to wear-out mechanisms.

These tests show that the D2W products examined in this report can provide a suitable energy-savings alternative to traditional incandescent lamps. The selected D2W products maintained the general robustness expected of SSL products: the first abrupt failure did not occur until 3,500 hrs of operation in the 6590 environment and only three parametric failures occurred before 3,500 hrs (there were 63 total DUTs). In addition, minimal changes to power consumption and TLA were observed. However, in addition to the failure mechanisms observed for other WTL products (e.g., secondary device optics changes), these tests revealed failure mechanisms unique to D2W products. Particularly, parametric failures (i.e., chromaticity shift [$\Delta u'v' \geq 0.007$], LFM < 0.70) were produced by improper current regulation to one or more LED primaries (due to control integrated circuit or logic failure modes) and degradation of red phosphors. As both current control and deep red phosphors are needed to mimic the deep dimming behavior of an incandescent lamp, this information is useful to future research aimed at reducing the impact of these failure modes on D2W device reliability.

Table of Contents

List of Figures

List of Tables

1 Introduction

The adoption of solid-state lighting (SSL) by commercial and residential users has continued to climb in recent years. The improved energy efficiency and reliability of SSL devices prompted the transition from traditional light sources to light-emitting diode (LED) sources. In the United States from 2008 to 2015, the number of residential installations of LED A-style lamps (the common “light bulb”) increased from less than 400,000 to more than 200 million [2]. As LED technology continues to develop, the cost reduction of SSL products and versatility of LEDs promote the adoption of LEDs in many new spaces. The ability to vary or tune the light spectra from an LED device has made the technology attractive to application-specific settings where human, plant, and animal wellbeing is directly affected and exploration into the benefits of LEDs has been studied in educational [3], medical [4], and horticulture [5] settings.

While the benefits of using LED over traditional light sources have increased over the past decade, some of the familiar aesthetics of traditional incandescent lighting were lost. For example, the emitted spectrum of an incandescent lamp changes to warmer correlated color temperatures (CCT) when it is dimmed, but when LEDs are dimmed, minimal change occurs to the emitted spectrum, resulting in a relatively stable CCT. This spectral change to warmer CCTs upon dimming is very attractive in residential, restaurant, theater, and other entertainment venues. For SSL devices to be fully realized in these spaces, manufacturers developed a new class of LED lamps designed to mimic the spectral behavior of incandescent lamps upon dimming while maintaining the energy efficiency of SSL products. These new products are termed “dim-to-warm” (D2W) or “warm-dimming,” and they are the focus of this report.

D2W lighting products are a subclass of white-tunable lighting (WTL) products and as such, the control architecture and overall design of D2W products mirror many of the features of WTL products as shown in **Figure 1-1**. The novelty of WTL devices is that the user can separately control the color and intensity of light emitted from the device through a user interface. The emission spectra (and subsequent color) of a WTL product is tuned between different CCT values by changing the amounts of electrical power supplied to

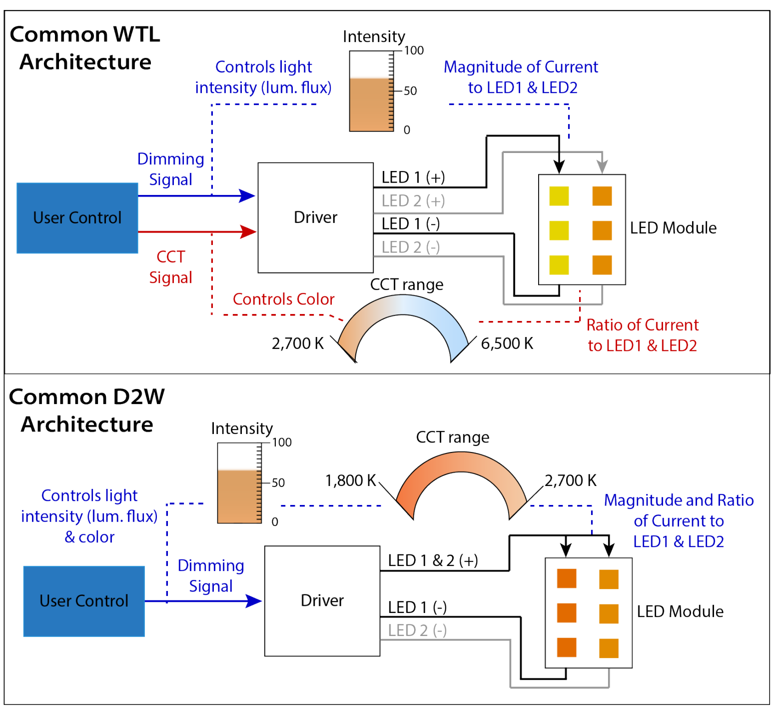

Figure 1-1. Schematic showing the common architectures for WTL products and their subset D2W products.

two or more LED primaries. In a traditional WTL product, one LED primary emits a low-CCT light (e.g., 2,700 K) and the other LED primary emits a high-CCT (e.g., 6,500 K) light. Many WTL devices are used in specific spaces (e.g., hospitals, offices, nursing homes) where both preset light conditions and the ability for the user to precisely adjust light color and intensity are useful. As such, many WTL devices use drivers that have independent channels for each LED primary so that spectral color and dimming level can be controlled separately.

As a subclass of WTL products, D2W products also tune the emission spectra between different CCT values by using two or more LED primaries. Since D2W products were designed to mimic incandescent lighting, a warmer color range is commonly chosen (e.g., 1,800 K – 2,700 K). The user interface for D2W lamps tends to be simpler than conventional WTL products because the end user predominantly cares that the emitted light appears "warmer" as the product is dimmed. As such, the dimming signal given by the user must be able to produce both appropriate CCT and dimming level. To achieve this, a driver with preset current levels and logic circuitry is commonly used to set the ratio and magnitude of current delivered to the two LED primaries. For the D2W devices, the current delivered to one LED primary directly affects the current delivered to the other LED primary.

In conjunction with the Next Generation Lighting Industry Alliance (NGLIA) and as part of the LED Systems Reliability Consortium (LSRC), RTI International procured a selection of commercially available D2W lamps and form factors. During the initial benchmarking phase, the lamps were disassembled and evaluated to understand the basic control architectures of D2W lamps and how these architectures affect dimming performance. The examined D2W lamps had two basic architectures. For both, only the warmest LED primary emitted light at deep dimming levels (i.e., when low power was supplied to the device) and at mid dimming levels (i.e., when an intermediate amount of power was supplied to the device), the higher CCT LED primary emitted light so that both LED primaries were on. The architectures differed at high power (i.e., no dimming), where some products turned off the warmest LED primary while other products continued to operate with all LED primaries emitting light. The performance of the D2W products (CCT dimming range, temporal light artifacts [TLA], spectral power distribution [SPD], and quality of light) were then compared to a traditional incandescent lamp [1].

The initial benchmark report was designed to understand where reliability issues may occur in D2W products and to guide the protocol needed to test these reliability concerns [1]. Like other WTL products, D2W products are subject to varying levels of reliability issues caused by optical material changes, chromaticity and luminous flux changes of LED primaries, and driver robustness. The level of these changes is impacted by the operating environment (e.g., temperature, humidity) and the amount of current delivered to each LED primary. In addition to these common WTL reliability concerns, the following areas were revealed as potentially specific reliability concerns for D2W products:

- Driver robustness: To aesthetically look like an incandescent lamp, D2W drivers must incorporate new logic circuits while maintaining a compact footprint to fit into the traditional A-style lighting infrastructure. The reliability of the new logic circuits and their effect on the reliability of the rest of the device is unknown.
- LED materials: The CCT range of D2W products is lower than traditional LED sources, and the degradation pathways leading to luminous flux loss and chromaticity shift are unknown.
- Dimmer compatibility: D2W products must be designed to work well with a variety of dimmers. As the device ages, it must maintain the same light quality with dimming.

This document is a follow-up report aimed at quantifying and understanding the reliability concerns of D2W products. This report uses accelerated stress test (AST) studies to collect sufficient data to research failure mechanisms and degradation of D2W products. This report focuses on the experimental findings and long-term trends of seven D2W products: four D2W lamp products (referred to as Lamp A – Lamp D) and three integrated LED solution products or LED modules (referred to as Module E, Module F, and Module G). The key parameters examined in this report include luminous flux, chromaticity maintenance, TLA (where applicable), and power of the D2W products. This document relates the trends seen in these key parameters to device architecture to provide and inform the lighting industry on the reliability and performance of this new class of D2W products.

2 Experimental and Analytic Methods

This report builds on our previous report about commercial D2W technologies that evaluated the different architectures in D2W products, assessed the dimming performance of those architectures, and provided initial characterizations for the products tested in this current report [1]. The experimental and analytic methods for this report are geared toward explaining the necessary tools to evaluate the experimental AST findings.

2.1 Samples

The commercially available devices under test (DUTs) examined in this study can be broadly categorized into two groups as described in our previous report [1]: lamps consisting of multiple LED packages of different CCT values and LED modules consisting of LED arrays in the chip-on-board (COB) or chip-scale package (CSP) format. Within each of these groups, a variety of subclasses and architectures exist.

2.1.1 Lamp A – Lamp D

Representative D2W lamps were chosen in two different styles: A-lamp and candelabra. The examined Lamp A – Lamp D and their initial characteristics, particularly their dimming performance compared to a traditional incandescent lamp, were described fully in our previous report [1] but an outline is provided briefly here in **Table 2-1** and **Figure 2-1**. In general, the D2W lamps emitted light in the correlated color temperature (CCT) range of 2,200 K to 2,700 K with a color rendering index (CRI) of at least 80. All lamps used two LED primaries,[1] but two different approaches were used to achieve D2W performance as outlined in Section 1. The lamps were tested as received in the temperature and environmental conditions.

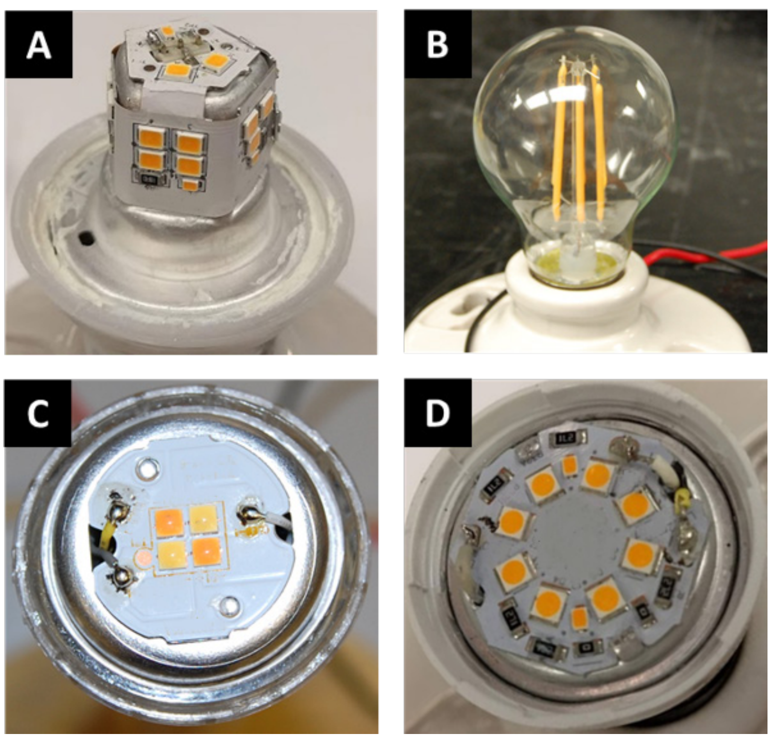

Figure 2-1. The D2W lamps examined during this study: (A) Lamp A, (B), Lamp B, (C), Lamp C, and (D) Lamp D.

[1] An LED primary is a group of LEDs of the same nominal CCT value that are connected together and operated in unison.

Table 2-1. Initial D2W Lamp Performance Characteristics.

Lamp ID	Lamp Type	Light Output (lm)	Input Power (W)	CCT (K)	CRI
A	A-lamp (standard)	800	9.5	2,200 – 2,700	80
B	A-lamp (filament)	800	8.5	2,200 – 2,700	80
C	Candelabra	345	5.0	1,800 – 2,700	90
D	Candelabra	450	5.5	2,200 – 2,700	80

The A-style lamps (Lamps A and B) had many similar key features: both were 60-W equivalent, had nominal light output of 800 lumens, and used two sets of mid-power LED (MP-LED) primaries to achieve lamp performance in the warm white CCT range (2,200 K – 2,700 K). However, the arrangement (standard LED module vs. filament style), number (26 surface-mounted LEDs vs. 138 LEDs arranged in 6 filaments), and size of the LEDs for Lamp A and Lamp B, respectively, were different as shown in **Figure 2-1** and discussed previously [1]. The candelabras (Lamps C and D) required similar input power to each other but varied substantially regarding light output, number and type of LEDs (4 LEDs vs. 10 LEDs), and D2W architecture (when no dimming was applied to the lamps, both LED primaries of Lamp C emitted light [Architecture 2] while only the higher CCT LED primary emitted light for Lamp D [Architecture 1]). The chromaticity points of the LED primaries for Lamps A – D are shown in **Figure 2-2** for clarity. A full analysis of dimming levels and their effects on SPD, power, and TLA for Lamps A – D is provided in **Appendix A**.

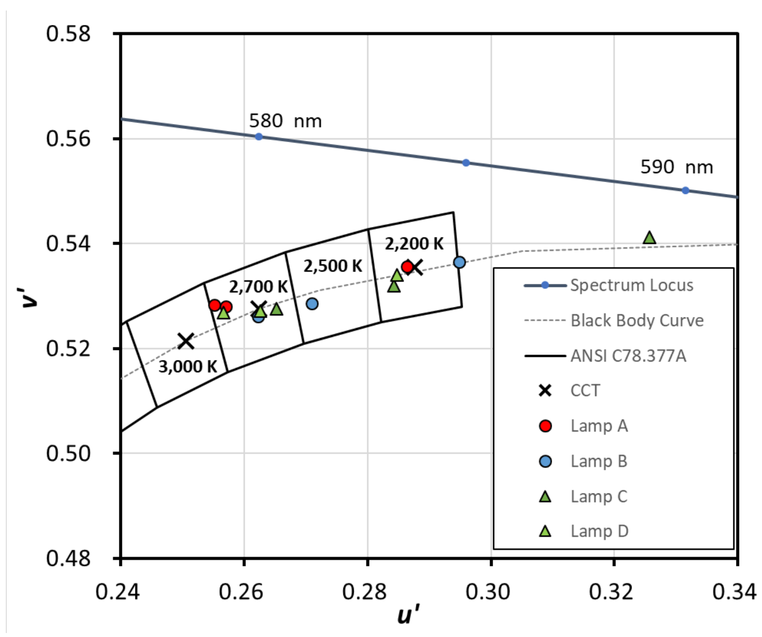

Figure 2-2. The chromaticity points (*u'* and *v'*) of Lamps A – D are plotted on the 1976 CIE diagram. The behavior approximates the black body curve as the lamps are dimmed from a starting point of approximately 2,700 K to between 1,800 – 2,200 K, depending on the product model. The relevant American National Standards Institute (ANSI) color bins as defined by ANSI C78.377A are provided as a guide.

2.1.2 LED Modules

Representative LED modules were chosen with COB and CSP form factors. Three different types of LED modules were examined in this work (Module E, Module F, and Module G) as shown in **Table 2-2** and **Figure 2-3**. The modules examined in this work have similar light output, input power, and CRI. Module E and Module F provided D2W performance in a low-CCT range (nominally 1,800 K – 3,000 K), which encompasses the CCT range of Lamps A – D. Module G provided D2W performance in a higher CCT range (nominally 2,700 K – 4,000 K) than the rest of the D2W technologies examined in this study, likely in an effort to provide a D2W analog for halogen lamps. Module E had 21 die mounted on a printed circuit board (PCB), and the die were covered with a phosphor-containing encapsulant (**Figure 2-3A**). Two different phosphor mixtures were patterned in the encapsulant for Module E; a darker orange phosphor strip down the center of the COB created the lower CCT emission (1,800 K) and a lighter orange phosphor on both sides of the strip provided the higher CCT emission. Module F and Module G both had six CSPs mounted to a PCB and the CSPs had two different phosphor formulations to provide higher and lower CCT primaries. The dimming method was similar for all three LED modules as discussed in our previous report [1]: all LEDs operated at high current and as the current was lowered, one or more LEDs were shut off until only the warm LEDs remained on at the lowest current settings. A full analysis of input direct current (dc) and how it relates to spectral and power changes for the LED modules is provided in **Appendix B**.

Table 2-2. Initial Characteristics of Integrated LED Solutions.

LED Module ID	LED Package	Light Output (lm)	Input Power (W)	CCT (K)	CRI
Module E	COB	565.2	6.2	1,823 – 3,020	95
Module F	CSP	514.7	5.5	1,778 – 3,046	90
Module G	CSP	533.5	5.5	2,672 – 4,009	92

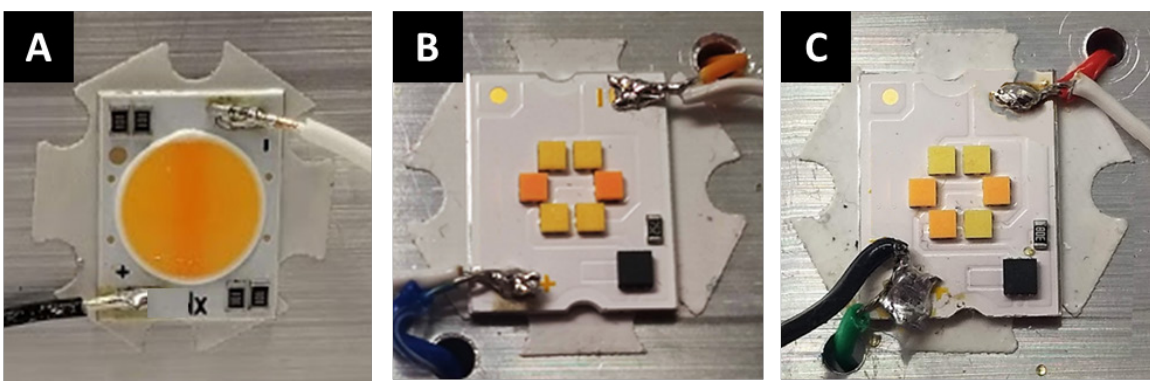

Figure 2-3. The D2W Integrated LED solutions examined in this study: (A) Module E, (B) Module F, and (C) Module G.

2.2 Stress Testing Methods

The samples of each type of lamp or LED module were separated into three populations consisting of three DUTs. There was one population for each of three conditions: room temperature operational life (RTOL), a temperature bake at a mildly elevated temperature of 45°C (45OL), and a temperature and humidity soak at 65°C and 90% relative humidity (6590). Either a temperature oven or a temperature-humidity environmental chamber was used for these tests. Humidity was not explicitly controlled in RTOL or 45OL, and the ambient humidity was determined by the air handling system of the building. All DUTs were power cycled as described later in this section.

For this study, the lamps were mounted in porcelain lampholders and operated upright. A single aluminum heat sink was used to mount three COB (or CSP) DUTs, making a COB (CSP) module, as shown in **Figure 2-4**. The COBs (CSPs) were wired in series so that the module could be operated by a single dimmable driver during testing, but they were also wired in a way that allowed them to be individually controlled by relay switches so that performance could be measured for individual COB/CSP samples. The drivers for the COBs (CSPs) were kept external to the test chamber and experienced only room temperature environments during testing.

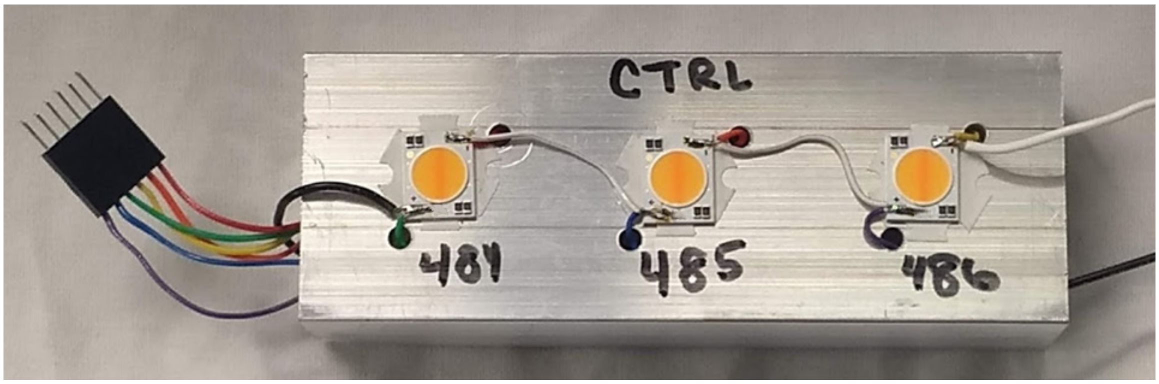

Figure 2-4. Test configuration for the Module E DUTs examined in this study.

2.2.1 Lamp Power Cycling

During all operational life tests, a Wink wireless control system consisting of a Wink Hub 2 and Z-Wave dimmers was used to set power (or dimming) levels for Lamp A – Lamp D. The Z-Wave dimmer is a phase-cut dimmer and, as explained in Section 2.1.1 and **Appendix A**, different dimming signal behavior was observed for the different lamps connected to the dimmer. Therefore, each lamp style (A – D) was controlled by a separate Z-Wave dimmer during power cycling. In general, setting the Z-Wave dimmer to 10% or 25% (deep dimming) activated only the lower CCT LED primary for the lamps, while setting the dimmer to 50% activated both lower and higher CCT primaries, giving an SPD with intermediate CCT. When the Z-Wave dimmer was set to 100% (no dimming), the higher CCT LED primaries were active and the lower CCT primaries were not active in some cases (Lamps A, B, and D); all LED primaries were active for Lamp C at 100% dimming. To maximize changes in temperature and CCT, the devices were power cycled through a repeating four-step dimming cycle of: 1) 100%, 2) 10% or 25%, 3) 50%, and 4) no power as shown in **Table 2-3**.

Table 2-3. Dwell Times at Each Dimming Level for Lamp A – Lamp D and the Total Time It Takes to Complete the Four-Step Process.

Lamp ID	Maximum Power (100%)	Low Power (10% or 25%)[a]	Mid Power (50%)	No Power (off)	Total Length of Dimming Cycle
A	30 mins	40 mins	32 mins	42 mins	144 mins
B	28 mins	32 mins	28 mins	32 mins	120 mins
C	40 mins	40 mins	50 mins	50 mins	180 mins
D	40 mins	46 mins	32 mins	42 mins	160 mins

[a] Low power was set to 10% for Lamp A and low power was set to 25% for Lamps B, C, and D.

The dwell time at each of the power settings in **Table 2-3** was customized for each lamp style to ensure that maximum thermal changes were achieved. To customize the dwell time, the thermal profile of the lamps were monitored with chromel/alumel thermocouples and the lamps were cycled through the four-step process at ambient room temperature; initial dwell times of 60 minutes were chosen because 60 minutes is normally sufficient time for LED junction temperatures to equilibrate at room temperature. When the dimming setting was changed, the lamp would warm up or cool down (depending upon whether it was going from low power to high power or high power to low power, respectively) and then plateau at a stabilized temperature (T_{stable}). To maximize the number of switching cycles in a 24-hour period, the dwell time at each dimming level was set to the amount of time it took for the temperature to reach 95% ($T_{95\%}$) of its stabilization temperature where $T_{95\%}$ was calculated according to Equation 2-1 and T_{start} represents the temperature just prior to switching the dimming level.

$$T_{95\%} = 0.95 \times (\mathrm{T_{stable}} - \mathrm{T_{start}}) \qquad \textbf{(Eq. 2-1)}$$

A representative thermal profile of one of the DUTs is provided in **Figure 2-5**. The $T_{95\%}$ temperatures at each dimming level are represented by red X's and the start time for each dimming cycle is highlighted with a vertical blue dashed line (**Figure 2-5A**). In **Figure 2-5B**, the temperature points are labeled for the switch from 25% dimming to 50% dimming. After the dwell times were calculated by this method, the dwell time at each dimming level was equally increased until the total minutes in the four-step process was a factor of the total minutes in a 24-hr period as shown in **Table 2-3**.

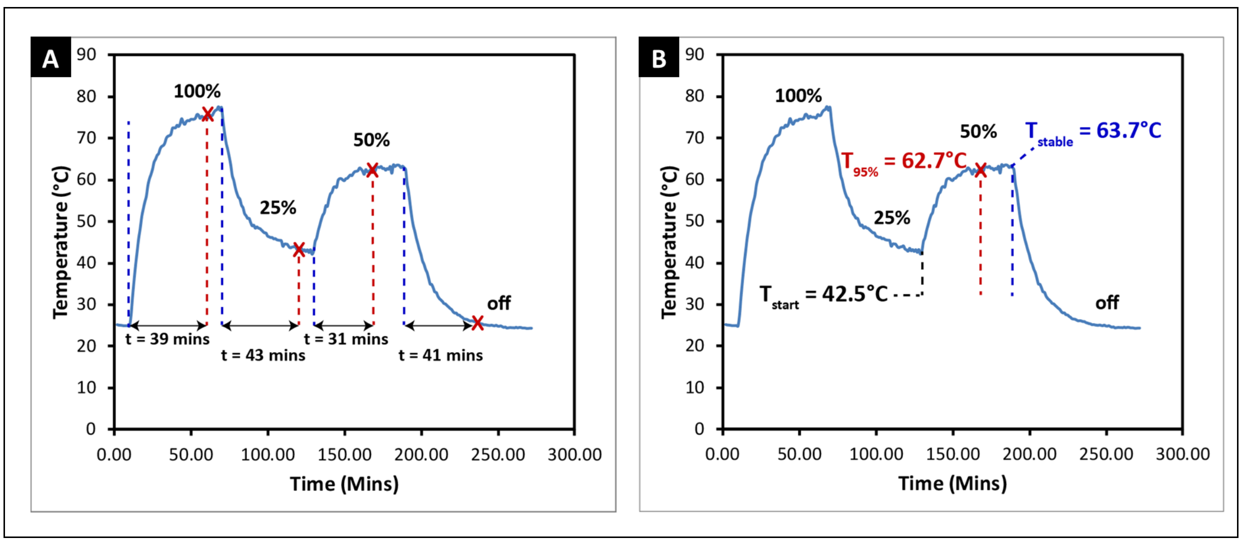

Figure 2-5. Thermal profile of a Lamp D DUT showing (A) start times (vertical dashed blue lines), $T_{95\%}$ (red X's), time at $T_{95\%}$ (vertical dashed red lines), and dwell time necessary to reach $T_{95\%}$ (horizontal double-sided black arrows with time labels), and (B) T_{start}, T_{stable}, and $T_{95\%}$ for the transition from 25% to 50% dimming.

2.2.2 LED Module Power Cycling

The LED modules (i.e., Module E, Module F, Module G) were also power-cycled with a four-step process: 1) high current, 2) low current, 3) medium current, and 4) no current (off). The behaviors of Module E, Module F, and Module G differed with input dc as shown in our previous report [1] and **Appendix B** of this report. Therefore, the input dc levels for "low," "medium," and "high" current settings were customized for each LED module to maximize changes in temperature and CCT as shown in **Table 2-4**. For all LED modules, the four-step power-cycling process repeated every 4 hrs, with each step operating for 1 hr before switching to the next step. During testing, dc was supplied to the COB (CSP) modules by Philips Xitanium dimmable LED drivers set on timers to maintain an accurate 4-hr loop.

Table 2-4. Current Levels Used During Power Cycling for the Integrated LED Solutions.

Integrated ID	High Current (mA)	Medium Current (mA)	Low Current (mA)
Module E	350	130	32
Module F	300	120	60
Module G	300	213	100

2.3 Measurement Methods

2.3.1 Luminous Flux

The SPD, luminous flux, and chromaticity measurements were obtained in a calibrated 65-inch integrating sphere with each sample mounted in the center of the sphere (4π geometry). Regular calibrations of the integrating sphere were performed using a calibrated spectral flux standard that was traceable to standards from the National Institute of Standards and Technology (NIST). Background corrections were applied prior to calibration. Self-absorption corrections were made for all samples by using an auxiliary lamp mounted inside the sphere, which is in accordance with procedures in the joint ANSI and Illumination Engineering Society (IES) standard ANSI/IES LM-79-19 [6]. Power was supplied to Lamp A – Lamp D using a designated Z-Wave dimmer, and SPDs were measured at two dimming levels: 100% and low power (10% or 25%). Constant dc power was supplied to the COB and CSP modules inside the integrating sphere using a Keithley 2400 SourceMeter, and external connections were made to operate only one COB (CSP) in the integrating sphere at a time. SPDs were measured at two input dc levels: high current and low current.

2.3.2 Flicker and Temporal Light Artifacts

Initial flicker and other TLA were measured for Lamp A – Lamp D using a handheld flicker meter mounted on a small integrating sphere placed over each DUT lamp. The measurements were made at low, medium, and max power settings (controlled by the Wink wireless system) using a handheld GigaHertz-Optik S-BTS256 spectral flicker meter. As shown in our previous report [1], the measured TLA metrics provide information on a lamp's compatibility with the chosen commercial dimmer (Z-wave dimmer) and do not necessarily reflect its compatibility with other dimmers. However, information about the degradation of the circuits necessary to provide D2W performance in the test lamps can be gained by observing the TLA metrics with time. Therefore, the TLA metrics of Lamp A – Lamp D were monitored as needed throughout testing. TLA metrics were not obtained for the COB and CSP DUTs.

2.3.3 Electrical Properties

Electrical properties (such as power consumption and power factor) of Lamp A – Lamp D were measured during photometric testing by using an electrical usage monitor on the ac mains. All measured electrical properties for Lamp A – Lamp D included power losses from the Z-Wave dimmer unless otherwise noted. For the COBs and CSPs, voltage measurements were obtained from the Keithley 2400 SourceMeter as it supplied input dc during photometric testing.

3 Results and Discussion

3.1 Lamp A – Lamp D

As originally reported, Lamp A – Lamp D were purchased in the summer of 2018 from local big-box retail stores. The initial SPDs from the lamps at low and maximum power (as defined in **Table 2-3**) are shown in **Figure 3-1**. The centroid wavelengths (λ_c) of the blue LED pump ($\lambda_{c,\ \text{blue LED}}$) and phosphor emissions ($\lambda_{c,\ \text{phosphor}}$) at both low and maximum power were calculated from the SPDs and are shown in **Table 3-1**. Aside from relative intensities, the lamp products have similar SPDs, with notable differences for the centroid wavelength of the blue LED pump for Lamp B and phosphor centroid wavelengths of Lamp C.

This section of the report discusses how the lamps age within the various ASTs and how the aging affects lamp SPDs and electrical performance. Section 3.1.1 discusses changes to luminous flux maintenance (LFM), Section 3.1.2 discusses chromaticity changes, Section 3.1.3 characterizes failure modes for the lamps, Section 3.1.4 evaluates changes to electrical power, and Section 3.1.5 assesses TLA metrics of the aged lamps. The data and results presented in this report are the average of populations of lamps at each respective AST condition. As mentioned in Section 2.1, the test population size for all lamps and LED modules started at three. Over the course of testing, seven lamp failures were observed. The test population (and data averaging) excluded failed lamps (abrupt or parametric failures) from the failure time onward.[2] Parametric failures were only excluded for the power level at which the failure occurred and in subsequent measurements. In this report, parametric failures are defined as samples that exhibited an LFM value below 0.70 or exhibited a chromaticity shift in excess of $\Delta u'v' \geq 0.007$.

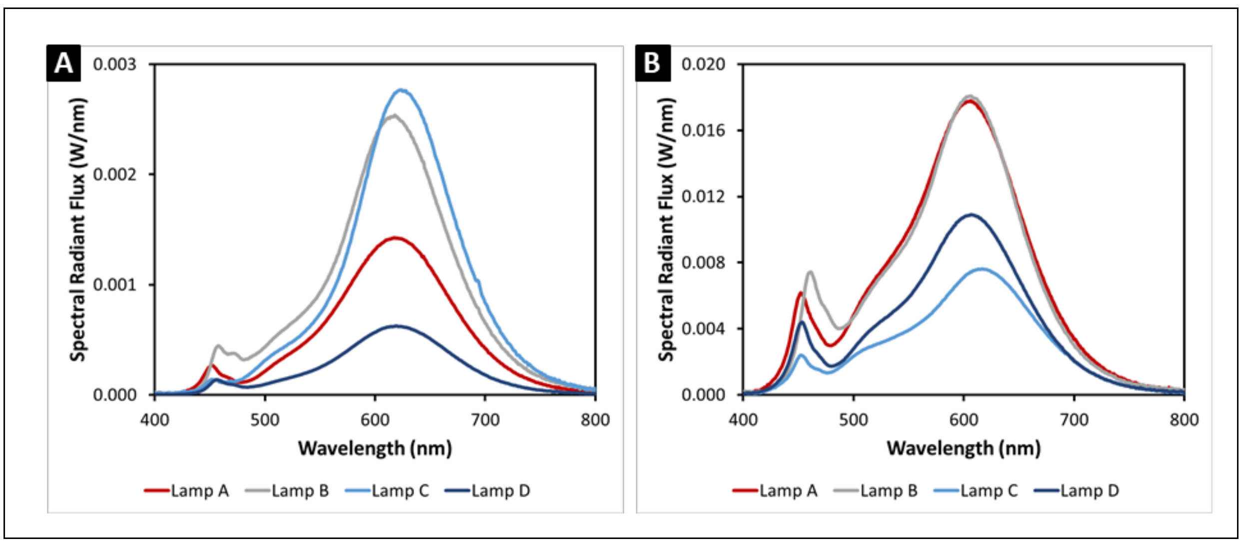

Figure 3-1. Initial SPDs of the control DUTs for Lamp A – Lamp D at (A) low power and (B) maximum power.

Table 3-1. Centroid Wavelengths of the Blue LED and Phosphors for Lamp A – Lamp D.

Lamp ID	$\lambda_{c,\ \text{blue LED}}$ (max power)	$\lambda_{c,\ \text{phosphor}}$ (low power)	$\lambda_{c,\ \text{phosphor}}$ (max power)
A	454.5 nm	617.9 nm	602.1 nm
B	459.7 nm	616.4 nm	601.3 nm
C	454.5 nm	625.9 nm	608.6 nm
D	454.4 nm	618.0 nm	603.2 nm

[2] Only sharp decreases in LFM or sharp changes to chromaticity were excluded from data averaging.

3.1.1 Luminous Flux Maintenance

Samples of each lamp type completed either 11,000 hrs of RTOL, 9,000 hrs of 45OL, or 7,000 hrs of 6590, and the LFM value of the lamps are shown in **Figure 3-2** and **Figure 3-3**. The A-style lamps (Lamp A and Lamp B) had generally high LFM values (above 0.80) at both low and maximum power at all AST test protocols (**Figure 3-2**) while the candelabra-style lamps had lower LFM (below 0.80) at the most aggressive AST test protocol (i.e., 6590 test conditions, see **Figure 3-3**).

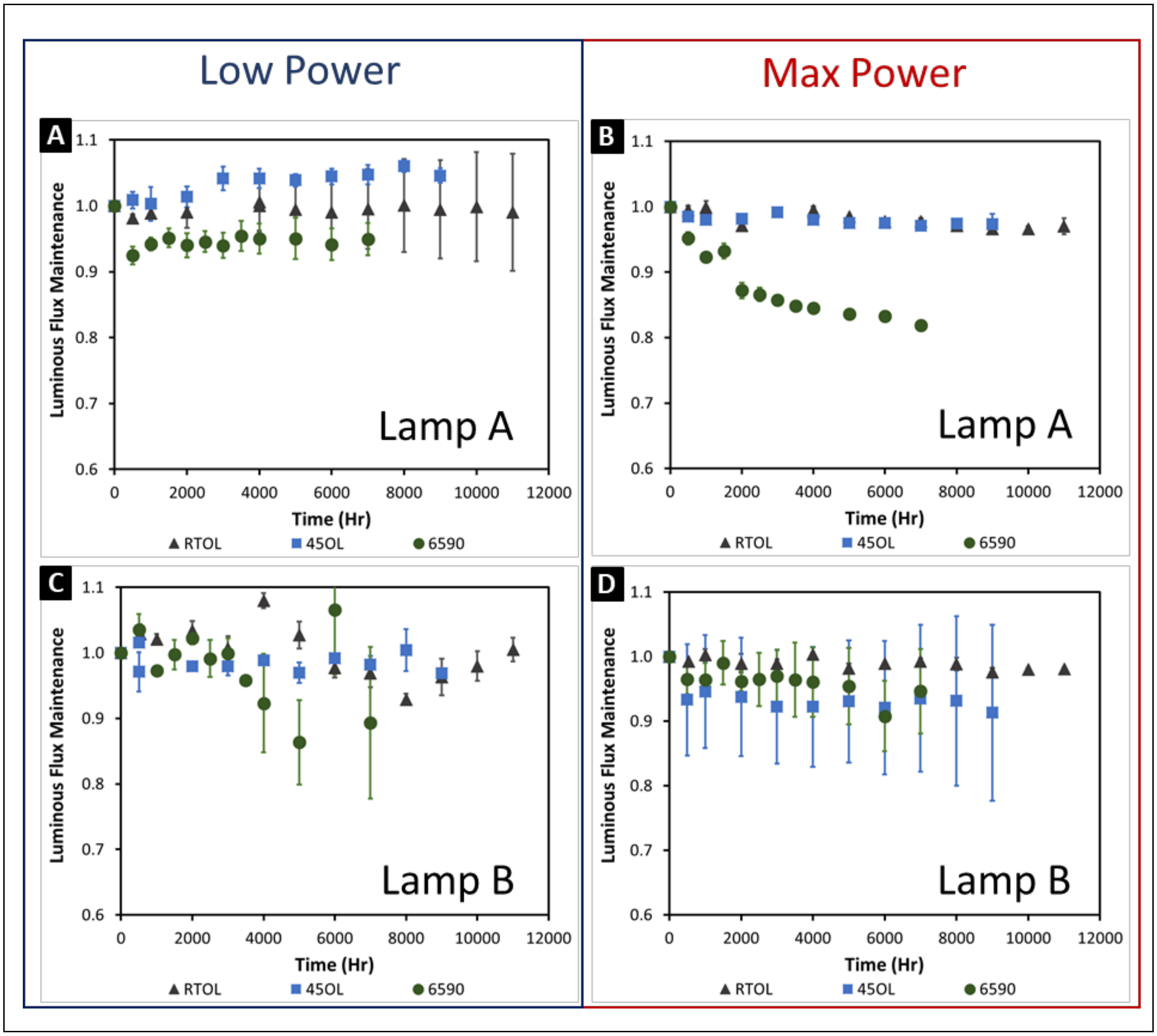

Figure 3-2. Average LFM for the populations of A-style lamps: (A) Lamp A at dimming to 10% power, (B) Lamp A at 100% power (i.e., no dimming), (C) Lamp B at dimming to 25% power, and (D) Lamp B at 100% power (i.e., no dimming).

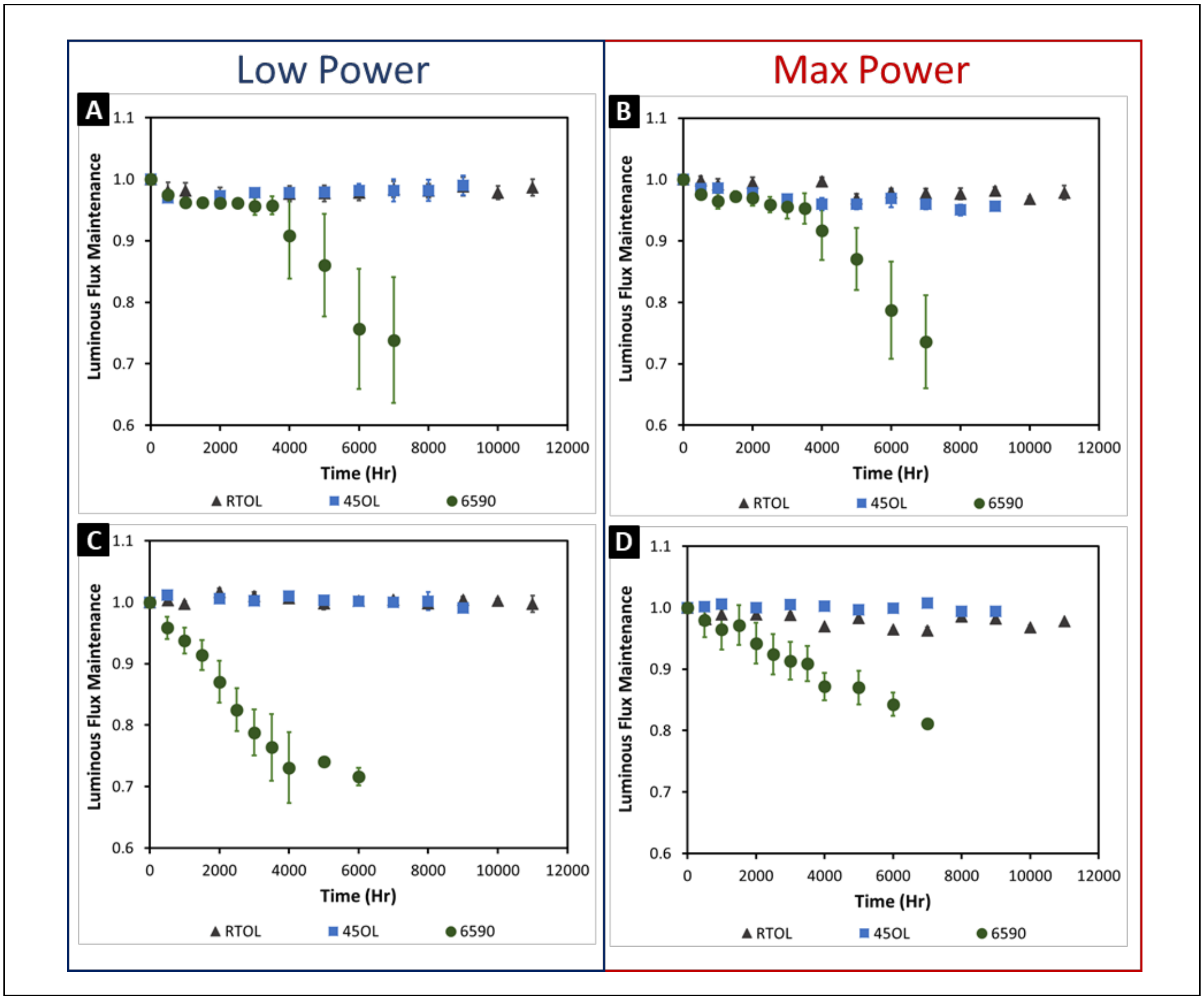

Figure 3-3. Average LFM for the populations of candelabra-style lamps: (A) Lamp C at dimming to 25% power, (B) Lamp C at 100% power (i.e., no dimming), (C) Lamp D at dimming to 25% power, and (D) Lamp D at 100% power (i.e., no dimming).

For Lamp A, LFM was statistically lower for DUTs operated in 6590 test conditions at both low and maximum power levels. There was no statistical difference in LFM between DUTs operated at RTOL and 45OL at either power level. In general, sample-to-sample LFM variation remained low for Lamp A DUTs throughout all ASTs as represented by the error bars in **Figure 3-2A** and **Figure 3-2B**. There was, however, one DUT (DUT 457, a Lamp A DUT) that behaved differently at low power than the other Lamp A DUTs operated at RTOL (its LFM dropped steadily to 0.88 while the other two DUTs maintained LFM above 1.03). DUT 457 was purchased about two weeks prior to the rest of the test population. As the gap between DUT 457's performance and the rest of the DUTs in RTOL widened, a fourth device was added to the RTOL test matrix. The fourth device (DUT 456) was purchased at the same time as DUT 457 and displayed similar LFM behavior to DUT 457 for the duration of its test period (5,000 hrs) as shown in **Figure 3-4.** The difference in performance between the two test populations could be a manufacturing flaw, a consequence of slight variations in components used, components manufacturer change, or a deliberate change in design by the lamp manufacturer. Further investigations of the root cause are not possible at this time without destroying the samples. No matter the cause, changes in dimming performance could impact end users to an undesirable level, and the researchers found that small purchase date changes (less than one month) also affected other lamps (e.g., the TLA metrics of Lamp D, not shown in this report). Effort was made to have homogeneous starting populations so that comparisons could be made across AST protocols and within AST protocols.

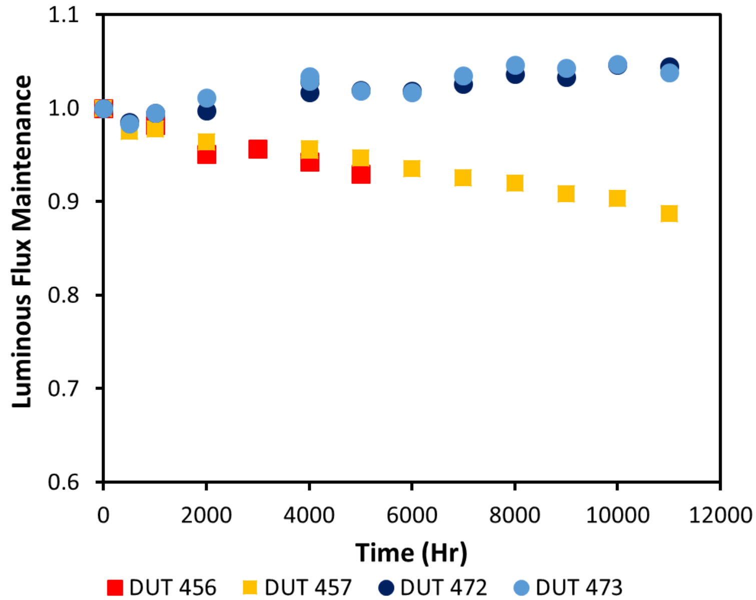

Figure 3-4. Luminous flux maintenance at low power for the Lamp A DUTs operated at RTOL show two test populations based on purchase date. DUT 456 and DUT 457 were purchased at the same time, and DUT 472 and DUT 473 were purchased two weeks later.

For Lamp B, the luminous flux of the control and DUTs varied greatly from test to test at the low power setting as shown in **Figure 3-2C**, suggesting some incompatibility between the electrical driver of the lamps and the Z-Wave dimmer. As a result of this incompatibility, it was difficult to assess how the testing conditions affected the warmer white LED primaries of Lamp B. Better stability with the Z-Wave dimmer was observed for the Lamp B DUTs at maximum power and average LFM remained high (LFM > 0.91 across all ASTs at max power as shown in **Figure 3-2D**). After only 500 hrs of testing at 45OL, one of the Lamp B DUTs (DUT 468) underwent parametric failure at low power (LFM = 0.26) and saw a great change in LFM at max power (LFM = 0.83). The LFM of DUT 468 was excluded from averaging at low power after 500 hrs but not max power (as the DUT was still operational at this power level), which led to the large standard deviation observed for 45OL devices at max power (**Figure 3-2D**).

Overall, the candelabra-style lamps (Lamp C and Lamp D) performed well in both RTOL and 45OL test conditions: LFM remained above 0.95 at both tested power levels and there was minimal sample-to-sample variation of LFM. The low sample-to-sample variation at all dimming levels was in part due to the good compatibility of the candelabra-style lamps with the Z-Wave dimmer. In the 6590 test, the LFM of the candelabra-style lamps was generally worse than the A-style lamps and average LFM fell below 0.80 for Lamp C DUTs at all power levels and Lamp D DUTs at low power. While the average LFM remained above 0.70 for both candelabra-style test populations operated in the 6590 test conditions, the LFM value of one Lamp C DUT dropped below 0.70 at all power levels by the end of test and all Lamp D DUTs underwent multiple parametric failures (some failed for excessive chromaticity shift and others were considered as failing due to LFM values below 0.70) before failing abruptly (one Lamp D DUT was operational at the end of test, but it was only operational at max power).

For the Lamp C DUTs operated in 6590 (**Figure 3-3A** and **Figure 3-3B**), there were two regions of LFM decay. The first was an incubation period through 4,000 hrs where LFM decay was slow with the decay rate similar to the devices operated at RTOL and 45OL. The second region of decay was faster and occurred from 4,000 hrs until the end of test. The slow and fast regions of decay observed in 6590 conditions for Lamp C were not observed at any other test condition or for any other lamp. Lamp C was the only lamp that used LEDs in the ceramic mid-power package, and it was also the only lamp with the electrical architecture where both LED primaries emit light at max power (i.e., when no dimming signal is applied). The two-step LFM decay may be package-related or, more likely, due to degradation of the different electronic architecture, but an exact cause remains unknown.

The decay rates for the Lamp D DUTs in the 6590 condition were stable over the test period (**Figure 3-3C** and **Figure 3-3D**). The slight increase in LFM at 5,000 hrs at low power for the Lamp D DUTs (**Figure 3-3D**) was the result of the DUT with the lowest LFM abruptly failing at this timepoint and being removed from averaging. The higher LFM observed for the maximum power setting for the Lamp D DUTs could suggest better stability of the higher CCT LED primary.

None of the testing protocols produced a sufficient drop in average LFM for L70 to be measured experimentally, so L70 values were projected using a modification of the TM-28-14 method [7].[3] LFM models for the DUTs of Lamp A – Lamp D at maximum power were determined from available experimental data, and the α values are shown in **Table 3-2** and the rated L70 values are shown in **Table 3-3**. The α values for Lamp A – Lamp D operated at RTOL and 45OL were generally small (less than 2×10^{-6}), and some of the α values were negative (Lamp C and Lamp D at RTOL) because LFM was still increasing through the end of test. These low α values project the time for LFM values to reach 0.70 beyond the three-times rule of TM-28-14,[4] suggesting high reliability, as measured by LFM, of the LEDs. As expected, projected L70 values for the lamps in the 6590 test conditions were lower overall, with the candelabra-style lamps having lower projected values than the A-style lamps. Lamp C had the worst projected L70 values while Lamp B's calculated lifetime exceeded the three-times rule. While these lifetime projections can be useful to determine LFM at a future time if the DUT is still operational, overall lamp system reliability should not be drawn from the projected L70 values. For example, two parametric failures were observed in 45OL conditions (a finding that is not predicted by the L70 projection), and two of the three Lamp D DUTs failed abruptly by 7,000 hrs in the 6590 test conditions (long before the L70 projection time of 12,312 hrs). Lamp system reliability is examined further in Section 3.1.3.

Table 3-2. Experimentally Derived α Values for Lamp A – Lamp D at Maximum Power.

Test	Lamp A	Lamp B	Lamp C	Lamp D
RTOL	2.82×10^{-6}	1.39×10^{-6}	-4.25×10^{-7}	-4.99×10^{-7}
45OL	1.16×10^{-6}	8.96×10^{-7}	1.78×10^{-6}	1.10×10^{-6}
6590	1.18×10^{-5}	8.16×10^{-6}	5.75×10^{-5}	2.84×10^{-5}

Table 3-3. Average Time to Reach L_{70} at Maximum Power for Lamp A – Lamp D.

Test	Lamp A	Lamp B	Lamp C	Lamp D
RTOL	> 33,000 hrs[a]	> 33,000 hrs[a]	> 33,000 hrs[b]	> 33,000 hrs[b]
45OL	> 27,000 hrs[a]	> 27,000 hrs[a]	> 27,000 hrs[a]	> 27,000 hrs[a]
6590	20,351 hrs	> 21,000 hrs[a]	8,174 hrs	12,312 hrs

[a] Limited by three times total test duration limit in TM-28-14.
[b] α value was negative, resulting in an infinite amount of time to reach L_{70}. Time was capped to three times the total test duration limit set by TM-28-14.

[3] This calculation ignores the facts that the lamps were power cycled during this test and not continuously operated as required by IES LM-84-14.
[4] The maximum projection time allowed by TM-28-14 varies depending on the number of samples in testing. For three samples, the maximum projection time is 3X [7].

3.1.2 Chromaticity

The chromaticity shift results for Lamp A – Lamp D are summarized in **Figure 3-5** for the A-style lamps and **Figure 3-6** for the candelabra-style lamps. These figures show the change in chromaticity from the initial point, where change is defined as $\Delta u'$ (the difference between u' at a given time and the initial value of u') and $\Delta v'$ (the difference between v' at a given time and the initial value of v'). In general, the average magnitude of the chromaticity shift ($\Delta u'v'$) for all lamp DUTs operated at RTOL and 45OL remained very low ($\Delta u'v' \leq 0.002$) during the test period examined in this report. The lamps evaluated during the 6590 test provided the clearest indication of the chromaticity shifts that can be expected to occur in the lamp products as they age, as this was the most aggressive test condition. Therefore, the chromaticity shift behavior of the DUTs operated at 6590 will be discussed more thoroughly in this section.

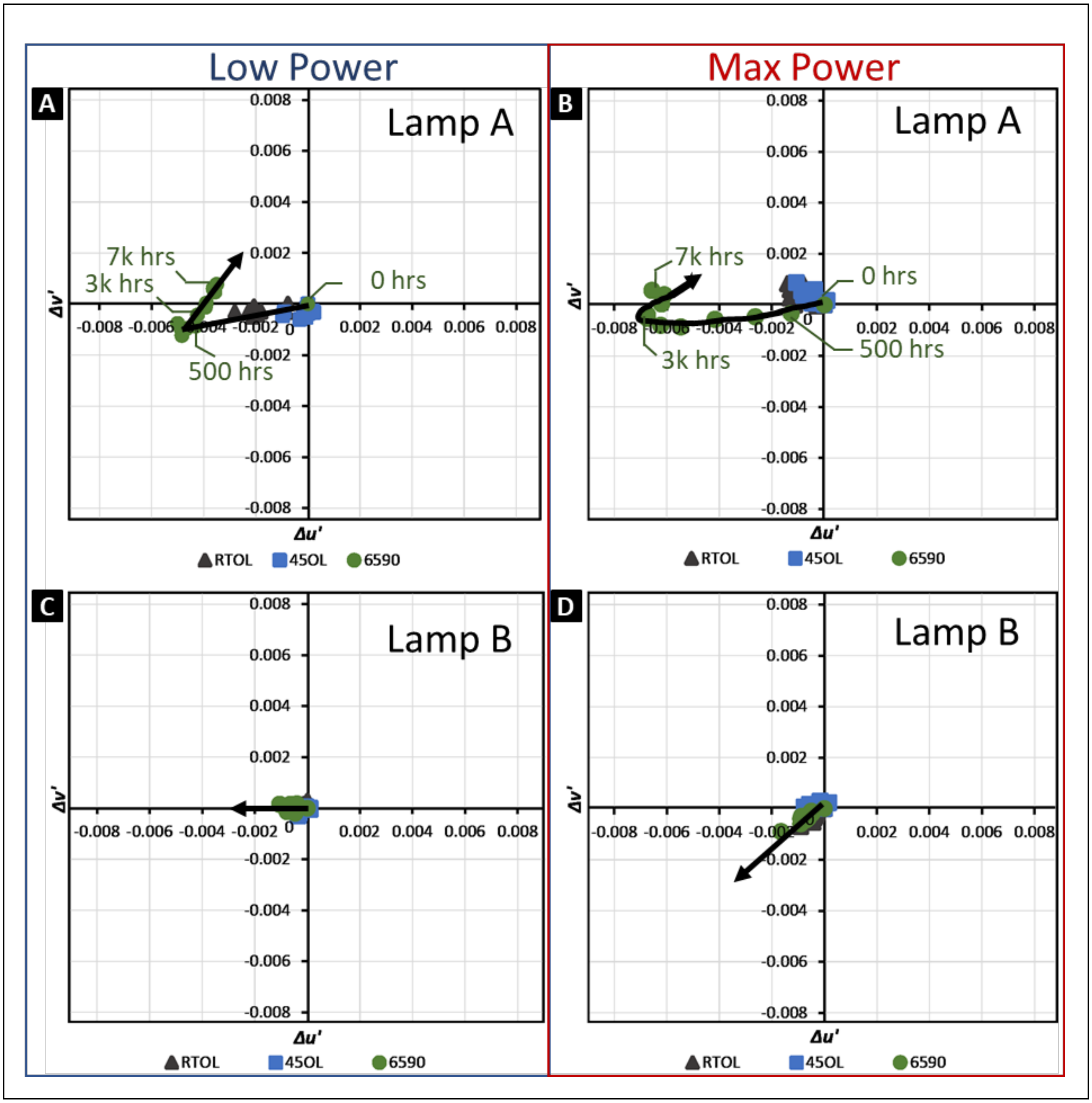

Figure 3-5. Chromaticity shifts for the A-style lamps in different ASTs: (A) Lamp A at low power, (B) Lamp A at maximum power, (C) Lamp B at low power, and (D) Lamp B at maximum power.

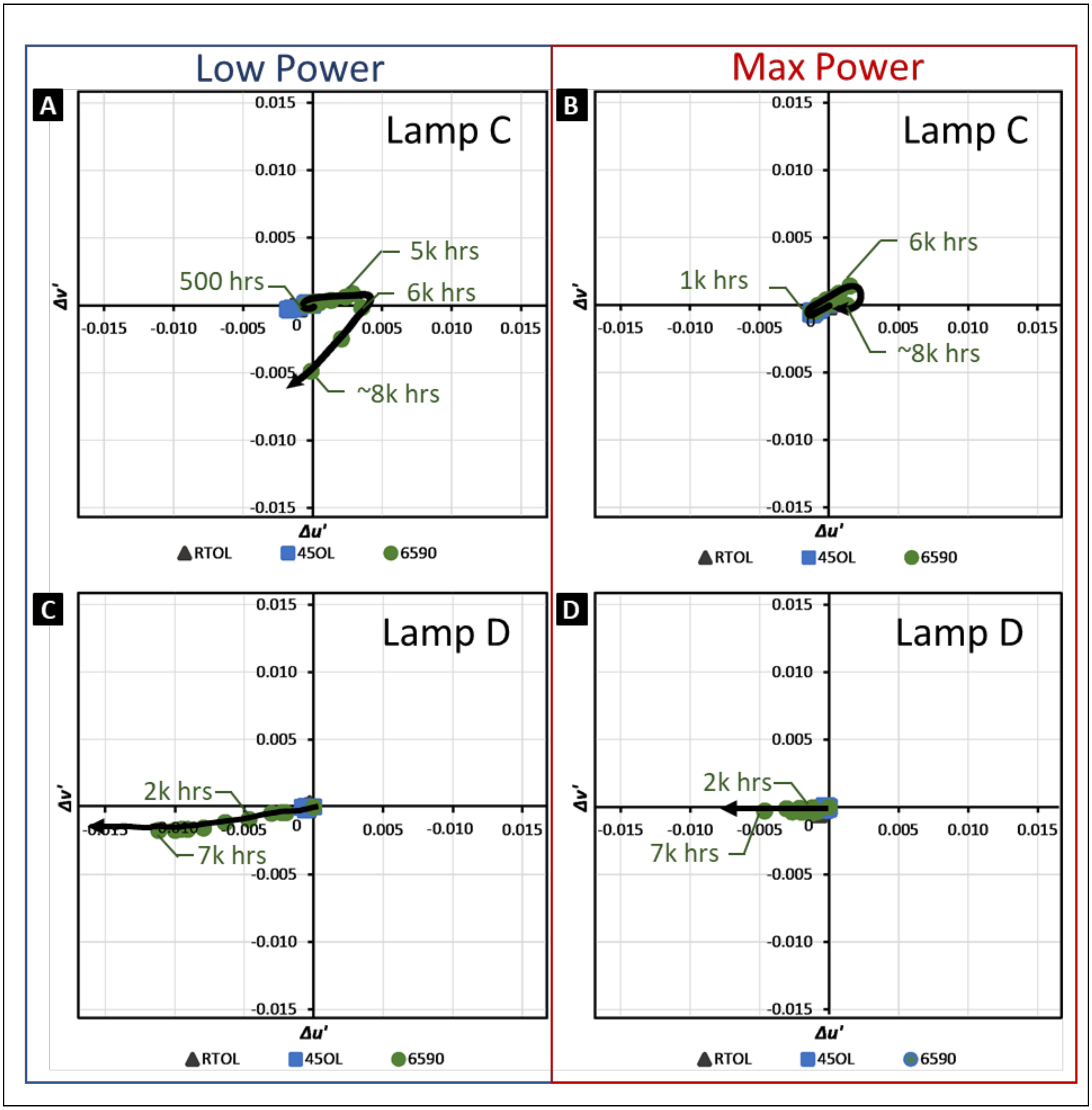

Figure 3-6. Chromaticity shifts for the candelabra-style lamps in different ASTs: (A) Lamp C at low power, (B) Lamp C at maximum power, (C) Lamp D at low power, and (D) Lamp D at maximum power. The Lamp C DUTs were operated in 6590 test conditions for 8,000 hrs.

The average magnitude of chromaticity shift for the A-style lamps (Lamp A and Lamp B) operated at 6590 remained acceptable ($\Delta u'v' < 0.007$) for the entire test duration examined in this study. Lamp A experienced greater chromaticity shift at all tested powers (low and max power) than Lamp B. The initial chromaticity shift for Lamp A DUTs operated in 6590 test conditions proceeded in the generally green direction (negative $\Delta u'$, mostly static $\Delta v'$). The timescale of the initial green shift was significantly different between the two LED primaries operating at low and max power (i.e., between the lower CCT and higher CCT LED primaries, respectively). The lower CCT LED primary abruptly shifted green to Δu = -0.0047 and Δv = -0.0010 after just 500 hrs (**Figure 3-5A**) while the higher CCT LED primary steadily shifted in the green direction to Δu = -0.0051 and Δv = -0.0010 in a time span of 2,000 hrs (**Figure 3-5B**). Green shifts are typically attributed to changes in phosphor composition. The steady green shift observed through 2,000 hours for the high-CCT LED primary was accompanied by a change in the phosphor peak position (> 2 nm) as shown in **Figure 3-7A**. It is likely that this shift in emission peak was the result of phosphor oxidation, which has been found in nitride phosphors [8]. The abrupt green shift observed for the lower CCT LED primary was not accompanied by a noticeable shift in emission peak (< 0.5 nm) but it was accompanied by a noticeable drop in luminous flux of the phosphor emission peak. The drop in phosphor luminous flux could lower the contribution of orange-red emissions and effectively raise the ratio of green emissions. After the initial green shift, the chromaticity coordinates remained relatively unchanged for a period before shifting in the red-yellow direction at both low and max power. A yellow shift is consistent with increased photo-oxidation of the globe which causes a shift in the blue LED centroid wavelength to longer wavelengths as shown in **Figure 3-7B**.

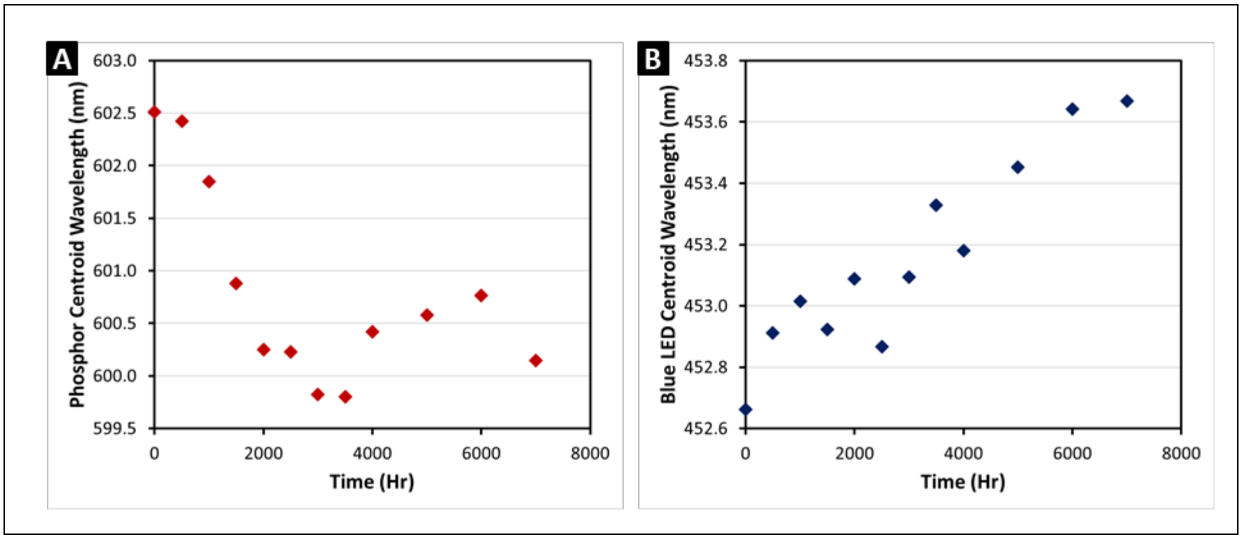

Figure 3-7. The centroid wavelengths of the higher CCT LED primary emitters of Lamp A steadily shifted during 6590 testing: (A) phosphor emission steadily shifted to lower wavelengths during the first 3,000 hrs and (B) the centroid wavelength of the blue LED shifted to longer wavelengths.

While the initial emissions generated from the phosphors for Lamp A and Lamp B were very similar (see **Figure 3-1**), aging in the 6590 conditions led to different behavior. The chromaticity coordinates of Lamp B remained relatively stable for the entire test. The lower CCT LED primary of Lamp B experienced a small green shift (Δu = -0.0011 and Δv = -0.0002, **Figure 3-5C**) and the higher CCT LED primary of Lamp B experienced a small shift in the green-blue direction (Δu = -0.0017 and Δv = -0.0009, **Figure 3-5D**). These shifts can be classified as CSM-2 and CSM-1, respectively, where CSM stands for chromaticity shift mode [9, 10]. These chromaticity shifts were not accompanied by noticeable shifts in the phosphor emission centroid wavelength. It is most likely that the difference in chromaticity shift between Lamp A and Lamp B was caused by the difference in lamp design. Lamp A used a traditional design consisting of a central LED module while Lamp B used a filament-style design where the LEDs were grouped into filaments. The filaments were designed to create an aesthetic look and mimic traditional incandescent lighting, and therefore the filaments were enclosed by a sealed glass bulb under positive pressure of an inert gas to create the desirable look [11]. The LEDs for Lamp A were enclosed by a plastic globe for light dispersion purposes and because of this, they were not held under positive pressure, making them more susceptible to oxidation. Consequently, the inert environment of the filament lamp likely restricted many degradation reactions for the LEDs, whereas the open environment of Lamp A readily permitted diffusion of oxygen and moisture into the LEDs, which could promote accelerated degradation. In addition, the surface temperatures of the globes of Lamp A and Lamp B were very similar at the three dimming levels, but the surface temperature near the electrical driver for Lamp A was higher than that of Lamp B at all dimming levels. Therefore, the propagation of heat from the electrical driver to the LED module of Lamp A might also be a source of the accelerated degradation of emission observed for the Lamp A DUTs.

For the candelabra-style lamps operated in the 6590 test conditions, the magnitude of chromaticity shift was acceptable at both low and max power settings for Lamp C DUTs ($\Delta u'v' < 0.0049$), but exceeded acceptable limits at low dimming levels in 6590 for the Lamp D DUTs. The chromaticity shift for the Lamp C DUTs was complex and likely dominated by different processes, changing the relative ratio of blue to red emissions throughout the test as shown in **Figure 3-8**. The chromaticity shift initially proceeded in the green and green-blue direction at low (**Figure 3-6A**) and max (**Figure 3-6B**) power, respectively. The initial shifts were small ($\Delta u'v' < 0.0015$), complete by 1,000 hrs, and likely caused by an immediate drop in phosphor emission at both dimming levels. After the initial green shift, the chromaticity started shifting in the generally red direction (positive $\Delta u'$, mostly static $\Delta v'$). The latter red shift passed back through initial chromaticity coordinates at both low and max power and continued along the positive $\Delta u'$ axis at low power; it continued in the positive $\Delta u'$ and positive $\Delta v'$ direction at max power. These red shifts were likely dominated by blue emission loss due to photo-oxidation of the globe (evidenced by blue LED centroid wavelength shifts to longer wavelengths, not shown). This blue emission loss was more prevalent in the higher CCT LED primary where more blue emissions occurred (i.e., at max power). After 6,000 hrs of operation in the 6590 test conditions, the chromaticity shifted in the blue-green and green direction at low and max power, respectively. The magnitude of this terminal blue-green shift was greater at the low power setting, and this might indicate that a new red phosphor degradation pathway began at this timepoint.

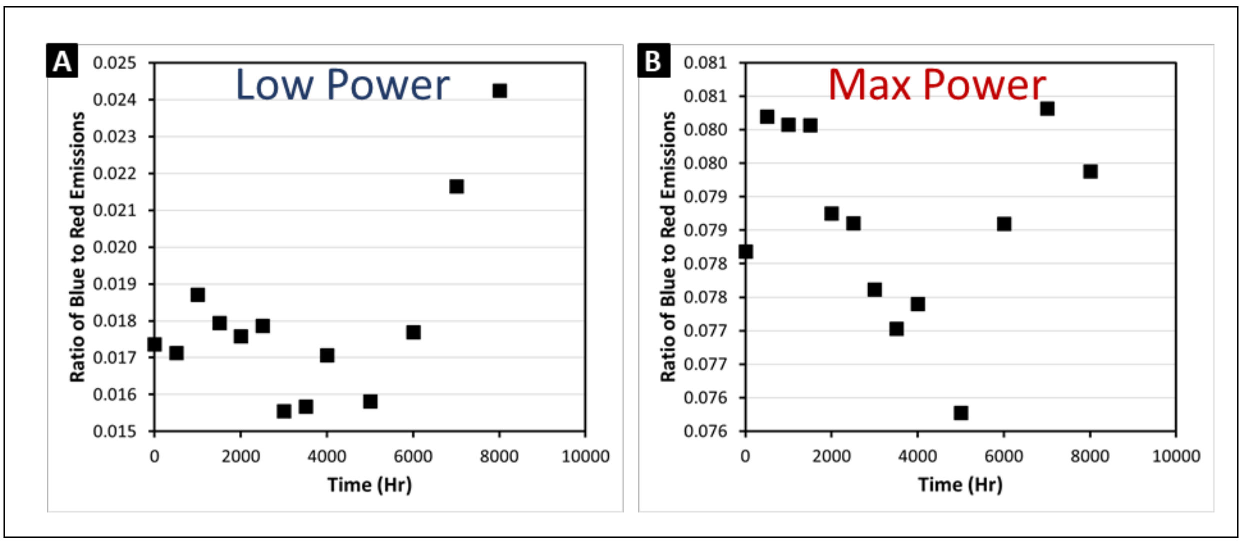

Figure 3-8. Different degradation pathways likely dominated the emission behavior of the Lamp C DUTs throughout testing, which led to varying ratios of blue to red emission at both (A) low power and (B) max power.

For the Lamp D DUTs operated at 6590, the chromaticity shift proceeded in the green direction for the entire test period at both low and max power settings as shown in **Figure 3-6C** and **Figure 3-6D**, respectively. The magnitude of the chromaticity shift for Lamp D DUTs operated in 6590 conditions exceeded acceptable limits ($\Delta u'v' \geq 0.007$) at low power by 3,000 hrs but remained within acceptable limits at max power. The chromaticity shift at low power was accompanied by a change in phosphor centroid wavelength position of the low-CCT LED primary toward green wavelengths. The change in centroid wavelength was greater than 3 nm and was likely a major contributor to the chromaticity shift change. The chromaticity shift at max power was not accompanied by a change in the phosphor peak centroid wavelength of the higher CCT LED primary for two of the three DUTs. Therefore, it is likely that the lower CCT LED primaries were more affected by oxidation than the higher CCT LED primaries in the Lamp D DUTs, and that this extra susceptibility combined with lower phosphor emissions with aging relative to blue LED emissions led to chromaticity shift failure of these lamps at low power.

3.1.3 Failure Analysis of Lamp A – Lamp D

In all, only 7 of the 36 DUTs (there were nine DUTs for each lamp model [A – D] at three test conditions [RTOL, 45OL, 6590]) failed parametrically or abruptly by the end of test. Three of the DUTs underwent complete abrupt failure at all power levels while a fourth experienced abrupt failure only at low power (all abrupt failures occurred for DUTs in the 6590 test conditions). Three of the DUTs only failed parametrically by the end of test, and these parametric failures were defined as the DUT having low LFM (e.g., below 0.70) or extreme chromaticity shift ($\Delta u'v' \geq 0.007$). The failure description, AST conditions, and time to failure for each failed lamp are summarized in **Table 3-4**.

Two of the seven failures occurred for the A-style lamps (Lamps A and B). While Lamp B outperformed its counterpart Lamp A in terms of average LFM and chromaticity shift (see **Figure 3-2** and **Figure 3-5**, respectively), both A-style failures occurred for Lamp B DUTs. The LFM value of Lamp B DUT 468 dropped below 0.70 at low power after just 500 hrs of testing in 45OL. The light output from the lower CCT LED primaries of DUT 468 dropped to about 30% after 500 hrs and remained there through the rest of test, suggesting a control integrated circuit (IC) communication failure early on in testing. Lamp B DUT 502 failed abruptly after 3,500 hrs of testing in 6590. The LFM measurement taken just prior to failure for DUT 502 was high (0.98) with no signs of an impending failure. Component analysis of DUT 502's electrical driver revealed a blown fuse. The cause of this fuse failure was unable to be determined and little sign of degradation on the PCB was observed.

Table 3-4. Lamp Failure Descriptions.

Lamp ID	DUT	AST	Failure Type – Power Level	Time to Failure (hr)
B	468	45OL	Parametric (LFM < 0.70) – Low Power	500
B	502	6590	Abrupt – Low Power Abrupt – Max Power	3,500
C	489	45OL	Parametric (chromaticity shift) – Max Power	7,000
C	508	6590	Parametric (LFM < 0.70) – Low Power Parametric (LFM < 0.70) – Max Power	6,000 7,000
D	500	6590	Parametric (chromaticity shift) – Low Power Parametric (LFM < 0.70) – Low Power Abrupt – Low Power Abrupt – Max Power	2,500 4,000 5,000 6,000
D	501	6590	Parametric (chromaticity shift) – Low power Abrupt – Low Power Abrupt – Max Power	3,500 7,000 7,000
D	512	6590	Parametric (chromaticity shift) – Low Power Abrupt – Low Power Parametric (chromaticity shift) – Max Power	3,000 7,000 6,000

For the candelabra-style lamps, Lamp C had two DUTs experience parametric failure while Lamp D had three DUTs experience a progression of failures. For the parametric failures of Lamp C, DUT 489 had a large chromaticity shift in the blue direction ($\Delta u' = -0.0131$, $\Delta v' = -0.0036$) and an increase in luminous flux (from LFM = 0.98 to LFM = 1.06) at high power settings after 7,000 hrs of operation in the 45OL environment. The cause of failure appeared to be logic or IC-related, as more current was supplied to the higher CCT LED primary after failure occurred as shown in **Figure 3-9**. Lamp C DUT 508 underwent parametric failure at all power levels by 7,000 hrs of operation in the 6590 test environment, and this failure appeared to be caused by degradation of the emitters.

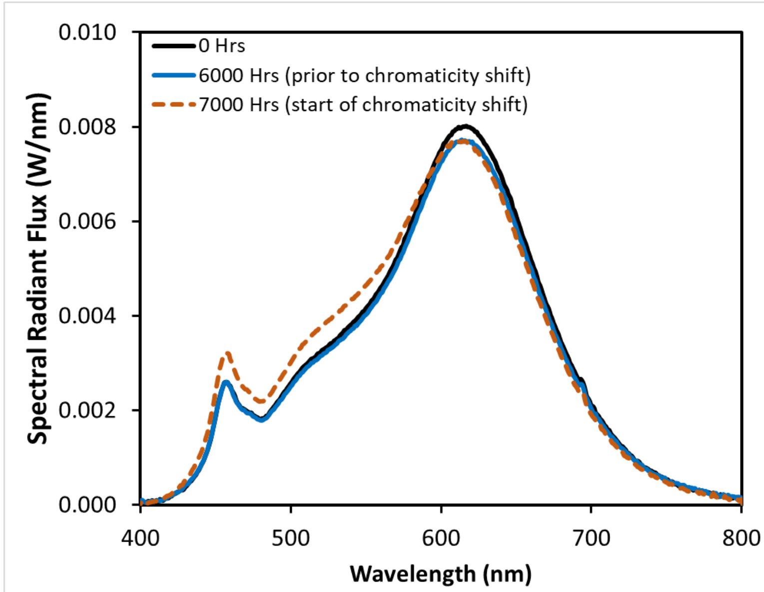

Figure 3-9. SPD of Lamp C DUT 489 at 7,000 hrs shows increased radiant flux in the blue region (450 nm – 500 nm) relative to the starting SPD (0 hrs) and SPD taken at 6,000 hrs just prior to parametric failure.

All Lamp D DUTs operated in the 6590 environment failed parametrically or abruptly by the end of test at all power levels (**Table 3-4**). At low power levels, the DUTs experienced a progression of failure that started with chromaticity shift failure (complete for all DUTs by 3,500 hrs) and ended with abrupt failure where no light was produced by the lamp. As mentioned in Section 3.1.2, the change in centroid wavelength of the warm white LED primary, likely caused by oxidation of the phosphor material, was likely a major contributor to the chromaticity shift change. Both DUT 500 and DUT 501 experienced abrupt failure at max power by 6,000 and 7,000 hrs, respectively. For DUT 500 and DUT 501 at max power, a small amount of light (LFM ≈ 0.01) was emitted from the lower CCT LED primaries. As was shown in our previous report [1] and in **Appendix A**, only the higher CCT LED primaries should emit light for Lamp D when it is set to max power. To understand this behavior, the DUTs were disassembled and their electrical properties were studied.

The Lamp D electrical drivers showed some discoloration of the PCB and the outer plastic around the base of lamps was cracked as shown in **Figure 3-10A** and **Figure 3-10B**, respectively. However, the electrical drivers for these DUTs were encased in a potting material and visual inspection and component analysis did not reveal significant wear or a definite source of failure. Further inspection of the LED modules for these DUTs revealed discoloration on the positive side of the MP-LEDs and flaking of the PCB as shown in **Figure 3-10C**. Even with the discoloration and cracking, the level of wear of the LED modules and MP-LEDs were not suspected to be the cause of abrupt failure for the DUTs. A simple test was conducted to show that some type of logic failure on the electrical driver was the likely cause of failure for the Lamp D DUTs. In the test, the power delivered to each LED primary was measured at max, mid, and low power for the 6590 DUTs and a control sample. The LED modules of the 6590 devices were then attached to the electrical driver of the control sample and the power delivered to each LED primary was measured again. The data at max and low powers are summarized for DUT 501 and a control sample in **Table 3-5**. The data show that the electrical driver of DUT 501 delivers insufficient voltage to both LED primaries at low power when compared to the control sample. In addition, at max power, the electrical driver for DUT 501 supplies 11.91 V to the lower CCT LED primaries (much higher than the control and a sufficient turn-on voltage) but only 14.27 V to the higher CCT LED primaries (an insufficient turn-on voltage). So, instead of only the cooler CCT primaries operating at max power, only the warmer CCT primaries are producing light at a low level. However, when the LED module of DUT 501 is paired with the electrical driver of the control, the lower CCT and higher CCT LED primaries receive the appropriate voltage and current when compared to the control at both low and high power settings. Therefore, the fault is unlikely to reside in the LED module of DUT 501. With these data, we believe that the increased impedance across the driver led to some type of logic failure of the manufacturer's preset current threshold.

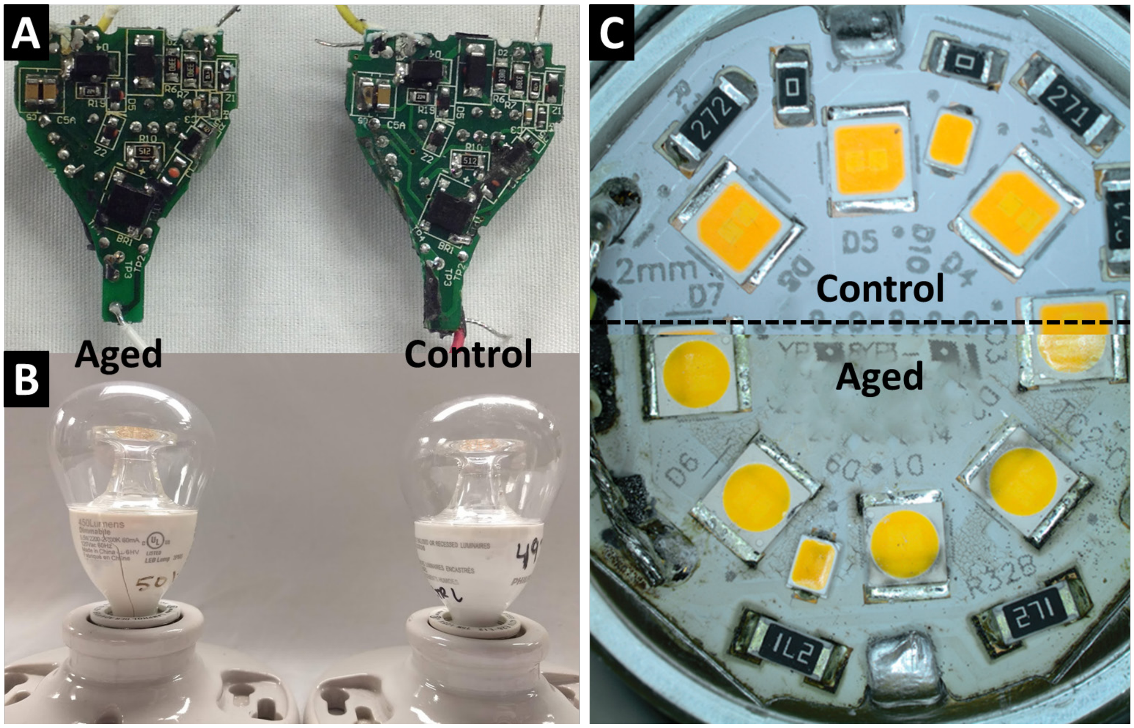

Figure 3-10. A representative Lamp D DUT aged at 6590 showing (A) minimal PCB discoloration, (B) cracking of the exterior plastics encasing the DUT, and (C) discoloration of the MP-LED terminals relative to the control DUT.

Table 3-5. Power Delivered to the Lower CCT (2,200 K) and Higher CCT (2,700 K) LED Primaries of a Lamp D Device (DUT 501) Post Abrupt Failure Compared to the Control Sample.

LED Primary	Electrical Driver	LED Module	Max Power (100% dimming)		Low Power (25% dimming)	
			Voltage (V)	Current (A)	Voltage (V)	Current (A)
Lower CCT	DUT 501	DUT 501	11.91	0.006[a]	6.42	0.002
Lower CCT	Control	Control	0.1	0.000[a]	18.1	0.026
Lower CCT	Control	DUT 501	0.1	0.000[a]	18.1	0.026
Higher CCT	DUT 501	DUT 501	14.27	0.005	7.36	0.002
Higher CCT	Control	Control	46.4	0.090	28.6	0.000
Higher CCT	Control	DUT 501	45.7	0.089	28.6	0.000

[a] The lower CCT LED primary should be off (i.e., zero current) at max power settings.

3.1.4 Electrical Analysis of Lamp A – Lamp D

In general, Lamp A – Lamp D were electrically robust, meaning that the lamps experienced minimal abrupt failures and minimal changes in power consumption and power factor for the duration of the testing period (11,000 hrs of RTOL, 9,000 hrs of 45OL, and 7,000 hrs of 6590). The change in power factor tended to be minimal for all lamps at RTOL and 45OL, and increased subtly for Lamps A, C, and D operated in 6590 test conditions. An increase in power factor with aging has been shown by us and others previously and is likely the cause of degradation of film capacitors in the EMI suppression circuit [12]. The change in power consumption for Lamps A, C, and D was also minimal (±0.1 W) throughout all ASTs and tested power levels. Therefore, luminous efficacy declined at a rate similar to the rate of luminous flux degradation for Lamps A, C, and D. Lamp B exhibited similar electrical behavior to Lamps A, C, and D at RTOL and 45OL but at 6590, Lamp B DUTs underwent a decrease in power consumption (from 8.2 W to 7.4 W) and power factor (from 0.78 to 0.74, not shown) at max power through 6,000 hrs as shown in **Figure 3-11A**. The ratio of decreased power consumption was greater than the luminous flux degradation (LFM ≈ 0.95, see **Figure 3-2D**). Therefore Lamp B DUTs operated at 6590 saw a minor increase in luminous efficacy over the duration of test as shown in **Figure 3-11B** despite having lower luminous flux.

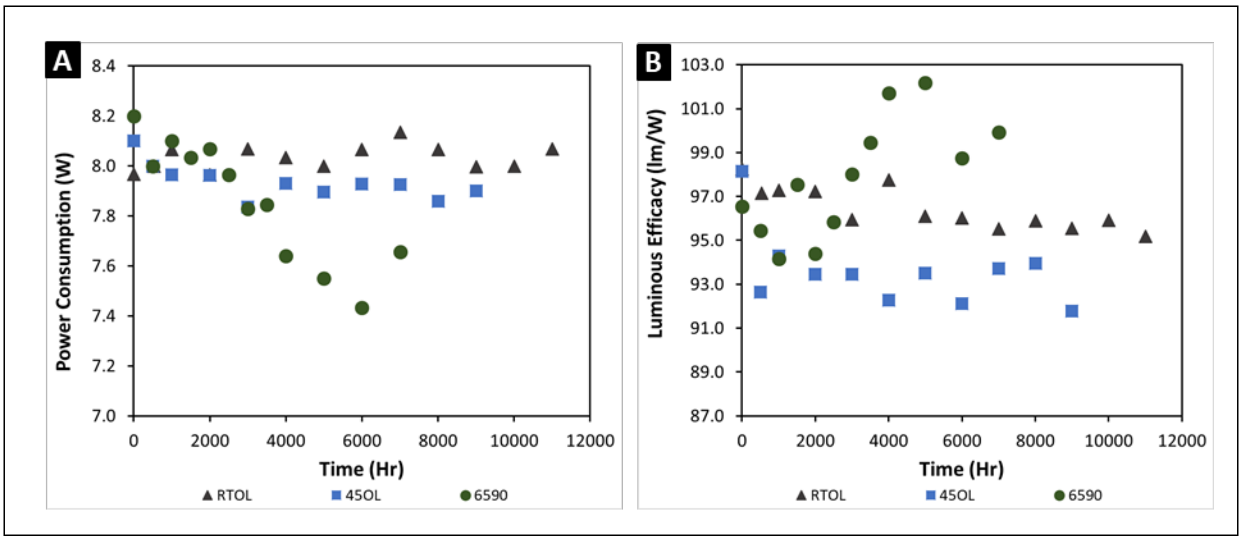

Figure 3-11. Average (A) power consumption and (B) luminous efficacy for Lamp B DUTs at max power.

3.1.5 TLA Metrics

The D2W lamps studied in this report used different driver architectures to adjust the relative brightness of the two LED primaries to maintain chromaticity near the black body curve while dimming. The driver architectures must maintain more than just chromaticity, as good electrical properties (e.g., high power factor and high efficiency) and high-quality visible light properties (e.g., low TLA) are just as valuable and can render the device unusable if they are not met. The behavior of the driver at each control voltage (dimming level) is preset by the manufacturer by circuit design or choice of control ICs, and dimming the LED lamp could cause an increase or induce fluctuation of luminance with time. These luminance fluctuations could be visible (e.g., flicker at light modulation frequencies up to 80 Hz and some stroboscopic effects between 80 Hz up to 2,000 Hz) or invisible to the end user, but the effects of the luminance fluctuations could be felt biologically (e.g., by causing headaches, visual impairment, seizures) and impact the user's wellbeing.

In our previous report [1], we analyzed the TLA behavior of Lamp A – Lamp D at low, mid, and max power when first operated. We found that the TLA behavior of each lamp was different at the different power levels. The stroboscopic visibility measure (SVM) and short-term flicker (P_{st}) values for the two A-style lamps (Lamp A and Lamp B) were below the recommended threshold of 1.0 set forth by the National Electronics Manufacturing Association (NEMA) 77-2017 standard [13], with Lamp B having better flicker, flicker index, SVM, and P_{st} values than Lamp A. For the two candelabra-style lamps (Lamp C and Lamp D), Lamp D had excellent flicker and TLA (with no detectable flicker at 25% dimming and below) while Lamp C had more TLA than the A-style lamps. The SVM values for Lamp C were above the recommended threshold of 1.0, but the P_{st} values remained below 1.0.

In this current report, we investigated how aging affected the TLA metrics for Lamp A – Lamp D. TLA characteristics of LED lamps are most often set by circuit design, so any aging of the driver components and circuits, especially those responsible for regulating and switching the LED primaries on and off, might produce undesirable TLA behavior. Because the 6590 AST conditions were the most aggressive, causing the most stress of driver components and circuits, TLA measurements of the functional DUTs that underwent 6590 AST for Lamp A – Lamp D were taken at the end of testing (7,000 hrs). The TLA metrics were then averaged and compared to the respective control device as shown in **Figure 3-12** through **Figure 3-15**.

For the A-style lamps, the frequency of flicker and shape of the flicker waveform generally did not change for DUTs operated in 6590 conditions for Lamp A (**Figure 3-12**) or Lamp B (**Figure 3-13**). There was an exception to this in that the flicker waveform shape at max power (100%) for Lamp B changed as the DUTs aged. For Lamp A DUTs operated in the 6590 test conditions, better TLA metrics were observed as the devices aged at all dimming levels. For Lamp B DUTs, generally higher percent flicker, flicker index, and SVM but lower P_{st} values relative to the control DUT were observed at all dimming levels. The reduced performance of the Lamp B DUTs with aging was still within accepted limits of the Institute of Electrical and Electronics Engineers (IEEE) 1789-2015 [14] and NEMA 77-2017 [13] standards. Even though the TLA metrics for Lamp A improved while the TLA metrics for Lamp B generally worsened, the performance of Lamp B relative to Lamp A was better at moderate and low dimming levels with the exception of P_{st}, which was better for Lamp A regardless of dimming level.

Lamp A

AST Conditions	TLA Metric	100%	50%	10%
Control	Percent Flicker (%)	13.4	29.4	5.9
	Index	0.042	0.074	0.014
	Frequency (Hz)	119.9	120.0	119.9
	SVM	0.441	0.781	0.131
	P_{st}	0.075	0.462	0.226
6590 (7,000 hrs)	Percent Flicker (%)	7.8	23.4	4.9
	Index	0.021	0.052	0.011
	Frequency (Hz)	120.0	119.9	120.0
	SVM	0.199	0.411	0.100
	P_{st}	0.037	0.052	0.183

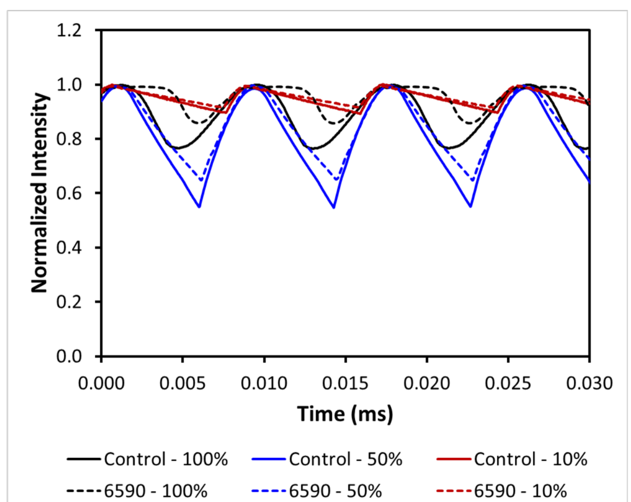

Figure 3-12. TLA measurements for Lamp A. The control DUT (solid lines) and the average TLA for DUTs operated in the 6590 conditions after 7,000 hrs (dashed lines) are compared in the graph and the resulting flicker percentage, flicker index, flicker frequency, SVM, and P_{st} are shown in the table.

Lamp B

AST Conditions	TLA Metric	100%	50%	25%
Control	Percent Flicker (%)	5.0	5.6	1.5
	Index	0.011	0.012	0.003
	Frequency (Hz)	119.9	119.9	119.9
	SVM	0.120	0.121	0.025
	P_{st}	0.248	0.108	0.671
6590 (7,000 hrs)	Percent Flicker (%)	11.8	6.0	1.9
	Index	0.030	0.014	0.004
	Frequency (Hz)	120.0	120.0	120.0
	SVM	0.287	0.132	0.034
	P_{st}	0.202	0.127	0.091

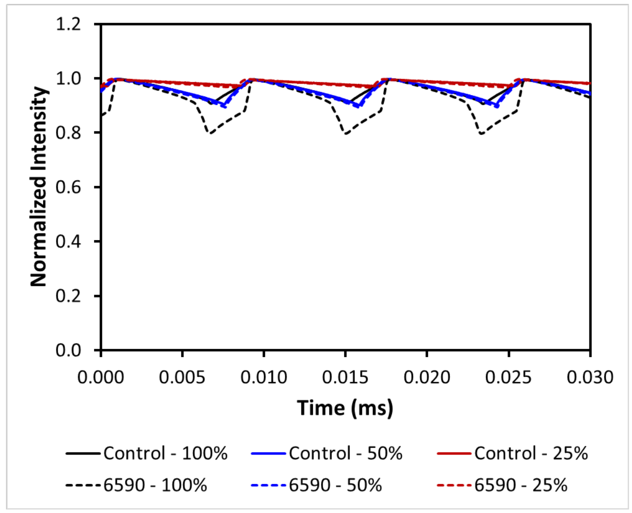

Figure 3-13. TLA measurements for Lamp B. The control DUT (solid lines) and the average TLA for DUTs operated in the 6590 conditions after 7,000 hrs (dashed lines) are compared in the graph and the resulting flicker percentage, flicker index, flicker frequency, SVM, and P_{st} are shown in the table.

As noted in this report and our previous report, Lamp C had the worst TLA performance of the lamps tested in this report. The cause of the poorer TLA performance for the lamp may have been the limited space available for the capacitor on the LED supply voltage line. As the Lamp C DUTs aged in the 6590 test conditions, minimal changes in the shape and frequency of the flicker waveform were observed through the end of test (7,000 hrs) as shown in **Figure 3-14**. However, the amplitude of the flicker waveform generally decreased with aging across all dimming levels, leading to better TLA metrics overall for the aged 6590 DUTs. Though the TLA metrics improved with aging, the SVM values remained higher than the recommended threshold of 1.0 at higher power levels (50% and 100%).

Lamp C

AST Conditions	TLA Metric	100%	50%	25%
Control	Percent Flicker (%)	43.7	59.7	40.0
	Index	0.120	0.191	0.104
	Frequency (Hz)	120.1	120.1	120.0
	SVM	1.330	2.078	1.068
	P_{st}	0.417	0.233	0.673
6590 (7,000 hrs)	Percent Flicker (%)	41.4	55.5	33.6
	Index	0.114	0.174	0.087
	Frequency (Hz)	120.0	120.0	120.0
	SVM	1.194	1.756	0.834
	P_{st}	0.329	0.261	0.470

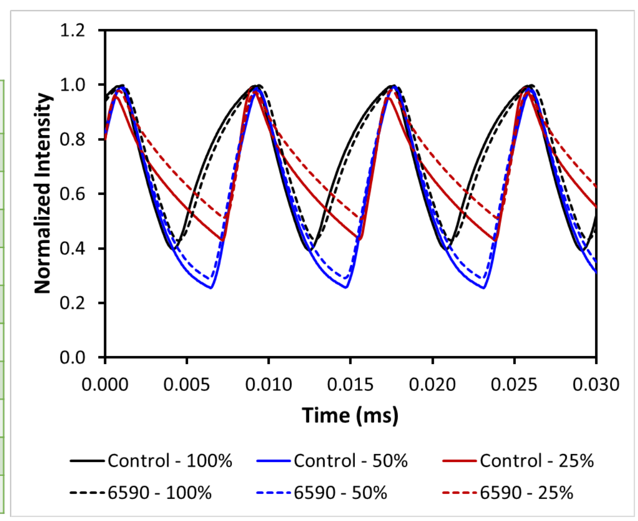

Figure 3-14. TLA measurements for Lamp C. The control DUT (solid lines) and the average TLA for DUTs operated in the 6590 conditions after 7,000 hrs (dashed lines) are compared in the graph and the resulting flicker percentage, flicker index, flicker frequency, SVM, and P_{st} are shown in the table.

Lamp D

AST Conditions	TLA Metric	100%	50%	25%
Control	Percent Flicker (%)	0.4	4.4	0.8
	Index	0.001	0.004	0.001
	Frequency (Hz)	119.9	120.0	104.9
	SVM	0.008	0.037	0.001
	P_{st}	0.330	0.179	0.298
6590 (7,000 hrs)	Percent Flicker (%)	14.7	45.7	11.7
	Index	0.047	0.126	0.019
	Frequency (Hz)	119.9	119.9	120.0
	SVM	0.487	1.327	0.188
	P_{st}	0.191	0.648	0.452

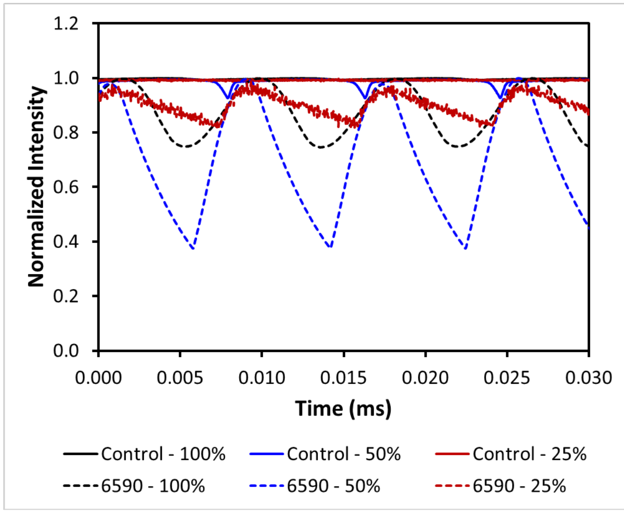

Figure 3-15. TLA measurements for Lamp D. The control DUT (solid lines) and the average TLA for DUTs operated in the 6590 conditions after 7,000 hrs (dashed lines) are compared in the graph and the resulting flicker percentage, flicker index, flicker frequency, SVM, and P_{st} are shown in the table.

At the end of test, only one Lamp D DUT remained functional in the 6590 test conditions (albeit the functional DUT parametrically failed at deep dimming levels [25%] due to low LFM). The flicker waveform and TLA metrics for the aged DUT were compared to the control DUT as shown in **Figure 3-15**. The flicker waveform of the aged DUT changed drastically at all dimming levels, and the percent flicker, flicker index, SVM, and P_{st} values generally increased significantly. Though the TLA values were sometimes as great as 50 times the control value, the TLA metrics for the aged DUT remained below acceptable thresholds established by NEMA 77-2017 (P_{st} = 1.0 or SVM = 1.0) at all dimming levels except 50% (SVM value).

3.2 COB and CSP LED Modules

The initial SPDs of the COB and CSP modules at low current and high current are shown in **Figure 3-16A** and **Figure 3-16B**, respectively. As described in Section 2.1, the white-tunable CCT ranges of Module E and Module F were similar (nominally 1,800 K to 3,000 K) while the white-tunable range of Module G was toward higher color temperatures (nominally 2,700 K to 4,000 K). Although Module E and Module F had similar CCT operating ranges, the centroid wavelength of phosphor emissions for Module E was red-shifted in comparison to Module F at both low and high current settings as shown in **Table 3-6**. As expected, the phosphor used for the higher CCT LED primary of Module G was blue-shifted in comparison to the phosphors used for Module E and Module F. The relative centroid wavelength locations of the blue LED pump remained similar across the COB and CSP modules.

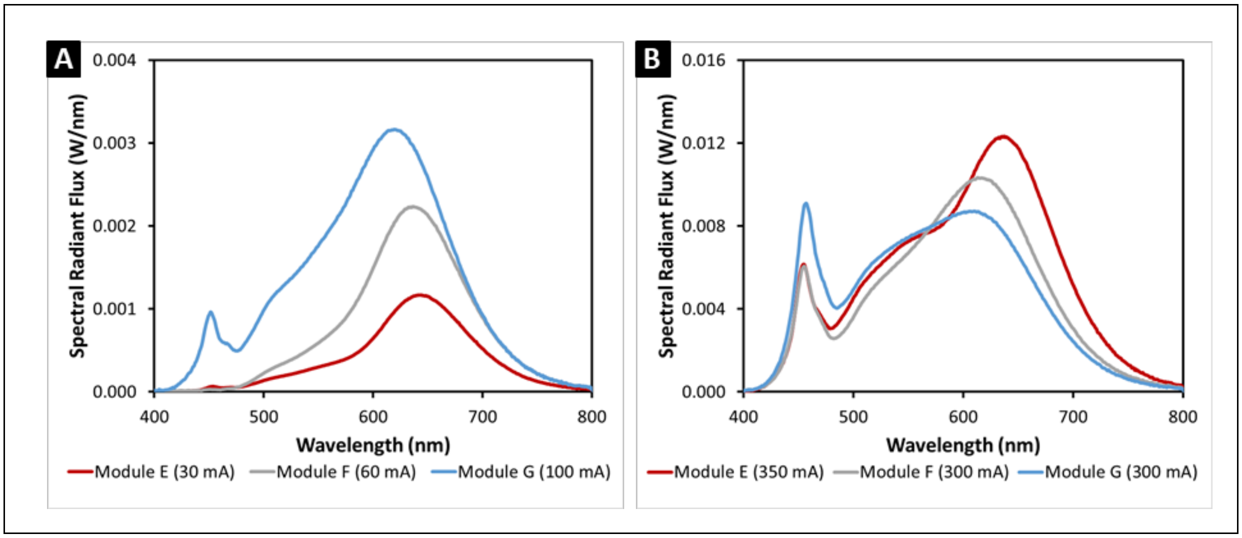

Figure 3-16. Initial SPDs of the LED modules at (A) low current and (B) high current.

Table 3-6. Centroid Wavelengths of the Blue LED and Phosphors for the Integrated LED Solutions.

Module	$\lambda_{c,\text{ blue LED}}$ (max current)	$\lambda_{c,\text{ phosphor}}$ (low current)	$\lambda_{c,\text{ phosphor}}$ (high current)
Module E	456.2 nm	636.2 nm	614.4 nm
Module F	455.9 nm	633.4 nm	605.6 nm
Module G	457.0 nm	609.1 nm	595.1 nm

The data and results presented in this report are the average of populations of Module E, Module F, and Module G at each respective AST condition. As mentioned in Section 2.1, the test population size for all lamps and LED modules started at three. Over the course of testing, four failures were observed for the LED modules. Two of the LED modules failed at all tested operating conditions (e.g., high current, low current), and the other two LED modules functioned regularly for some of the tested operating conditions. Additional details of these failures are found in Section 3.2.3. The test population (and data averaging) only excluded LED modules with parametric failures at the operation conditions for which they failed and subsequent measurements.

3.2.1 Luminous Flux Maintenance of LED Modules

The average LFM across the AST protocols at low current and high current for the LED module DUTs is shown in **Figure 3-17**. For the duration of tests in this report (7,000 hrs at RTOL and 45OL; 6,000 hrs at 6590), the average LFM for the LED modules remained greater than 0.85 for DUTs during all three stress protocols. Further, for DUTs operated at the two lower-stress protocols (RTOL and 45OL), the average LFM remained above 0.96. Examination of the LFM graphs in **Figure 3-17** shows higher standard deviations for measurements taken at high current as opposed to low current, which is especially evident for Module E and Module F (**Figure 3-17A–D**). The reason for this variability is unknown but could relate to higher degradation of logic components at high current levels due to higher localized heat at these settings.

For Module E, the average LFM for DUTs operated at RTOL and 45OL was very similar, while the average LFM for DUTs operated at 6590 was much lower (**Figure 3-17A** and **Figure 3-17B)**. Likewise for Module F, the average LFM for DUTs operated at RTOL and 45OL was very similar while the average LFM for DUTs operated at 6590 was much lower (**Figure 3-17C** and **Figure 3-17D)**. For Module G, the average LFM for DUTs operated at RTOL and 45OL was very similar at the low current setting (**Figure 3-17E**) but not at the high current setting (**Figure 3-17F**). At the high current setting for Module G, the rate of luminous flux decay changed and exhibited greater correlation with the AST protocols; lower LFM was observed for AST protocols with higher temperature stresses.

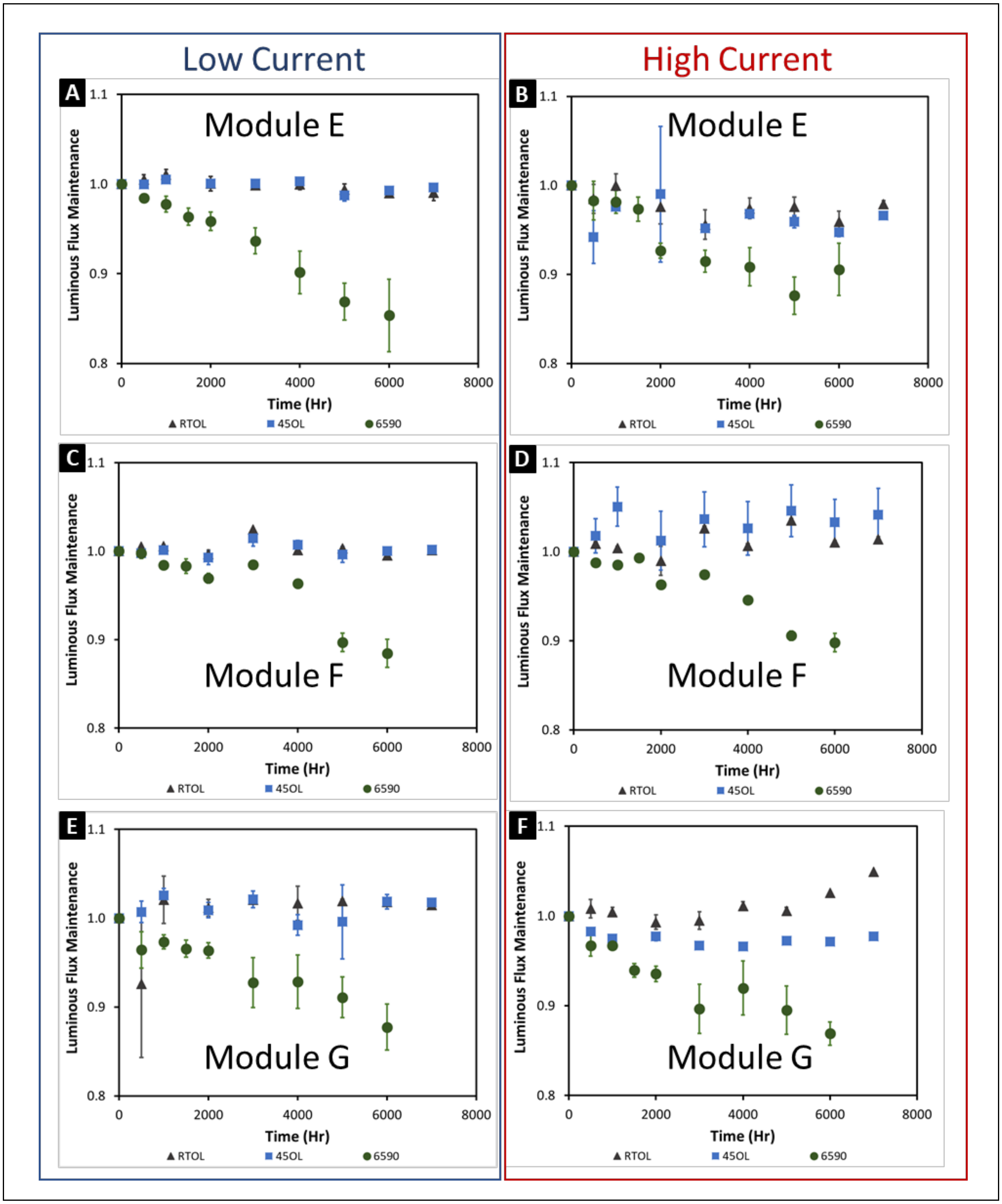

Figure 3-17. Average LFM for (A) Module E at low current, (B) Module E at high current, (C) Module F at low current, (D) Module F at high current, (E) Module G at low current, and (F) Module G at high current.

For all LED modules, the LFM could be modeled with a single exponential equation to determine the decay rate constants (α) in accordance with the modified IES TM-28-14 [7]. The α values obtained from these models at each AST protocol at high current are shown in **Table 3-7**. Because there are 7,000 hrs of data for RTOL and 45OL and only 6,000 hrs of data for 6590, the data between 2,000 and 7,000 hrs were used to calculate the LFM models for RTOL and 45OL, while the data between 1,000 hrs and 6,000 hrs were used to calculate the LFM models for the 6590 conditions. For the 6590 test conditions, single-exponential least squares fits of the data produced good coefficient of determination ($R^2 > 0.80$) for Module F and Module G and a moderate coefficient of determination for Module E ($R^2 = 0.68$). For the RTOL and 45OL test conditions, the coefficients of determination were generally low, suggesting that more data might be needed to accurately project lifetime at these conditions. The largest α value obtained was 1.94×10^{-5} (Module F at 6590 test conditions), and none of the testing protocols produced a sufficient drop in LFM for L70 to be measured experimentally. Therefore, this value must be projected using the TM-28-14 method. Because only three samples were used during this testing, projection times were limited to three times the actual test time per the rules of the modified IES TM-28-14 method [7]. Perhaps the most significant finding from the LFM models was that the projected time to reach L70 exceeded the threshold set by the three-times rule given in IES TM-28-14 at all AST protocols. The three-times projection limit is 18,000 hrs for 6590 test conditions and 21,000 hrs for RTOL and 45OL test conditions, suggesting high robustness. However, four parametric failures occurred before this projected lifetime as is discussed in Section 3.2.3.

Table 3-7. Experimentally Derived α Values for the LED Modules at High Current.

Test	Module E	Module F	Model G
RTOL	-7.97×10^{-7}	-2.91×10^{-6}	-1.03×10^{-5}
45OL	4.16×10^{-6}	-4.37×10^{-6}	-6.00×10^{-7}
6590	1.65×10^{-5}	1.94×10^{-5}	1.83×10^{-5}

3.2.2 Chromaticity Shifts of LED Modules

The chromaticity shifts for Module E, Module F, and Module G at low and high current settings are shown in **Figure 3-18**. Through the end of the tests, four LED module DUTs failed parametrically due to chromaticity shift. Two of these DUTs were the high-CCT LED module product (Module G), and these parametric failures occurred at all tested currents (both DUTs were operated at RTOL). The two other DUTs experienced chromaticity shift failure at only one of the tested current levels. These chromaticity shift parametric failures are discussed in more detail in Section 3.2.3.

Between the low-CCT products, Module E DUTs exhibited the largest chromaticity shift ($\Delta u'v' = 0.0043$ at 6,000 hrs of testing in 6590) as shown in **Figure 3-18A** and **Figure 3-18B**. At low current setting (**Figure 3-18A**), Module E DUTs exhibited CSM-2 behavior (i.e., the chromaticity shifted in the green direction along the $-\Delta u'$ axis with little change in $\Delta v'$). CSM-2 behavior can be caused by changes in phosphor material or by a reduction in red emissions. No peak shifts were observed for the Module E DUTs, but the red emissions peak was greatly reduced from its initial value after 6,000 hrs of 6590. At the high current setting (**Figure 3-18B**), the Module E DUTs exhibited CSM-1 behavior (i.e., chromaticity changed in the blue direction along the $-\Delta u'$ axis and $-\Delta v'$ axis with similar magnitude), which is generally caused by the stability of the blue LED pump in comparison to phosphor materials. These chromaticity shifts for Module E were consistent with the chromaticity shifts seen in the lamp products studied in this report (Section 3.1.2).

The Module F DUTs exhibited moderate chromaticity change ($\Delta u'v' = 0.0041$) at low current setting and small chromaticity change ($\Delta u'v' = 0.0013$) at high current setting by the end of 6,000 hrs of testing in 6590 as shown in **Figure 3-18C** and **Figure 3-18D**. Though the magnitudes of the shifts were so small at all AST test conditions through 4,000 hrs (i.e., the shifts were near the limit of detection), data collected in the 6590 test conditions after 4,000 hrs suggests that chromaticity shift will continue to proceed in the green direction (CSM-2) for these DUTs.

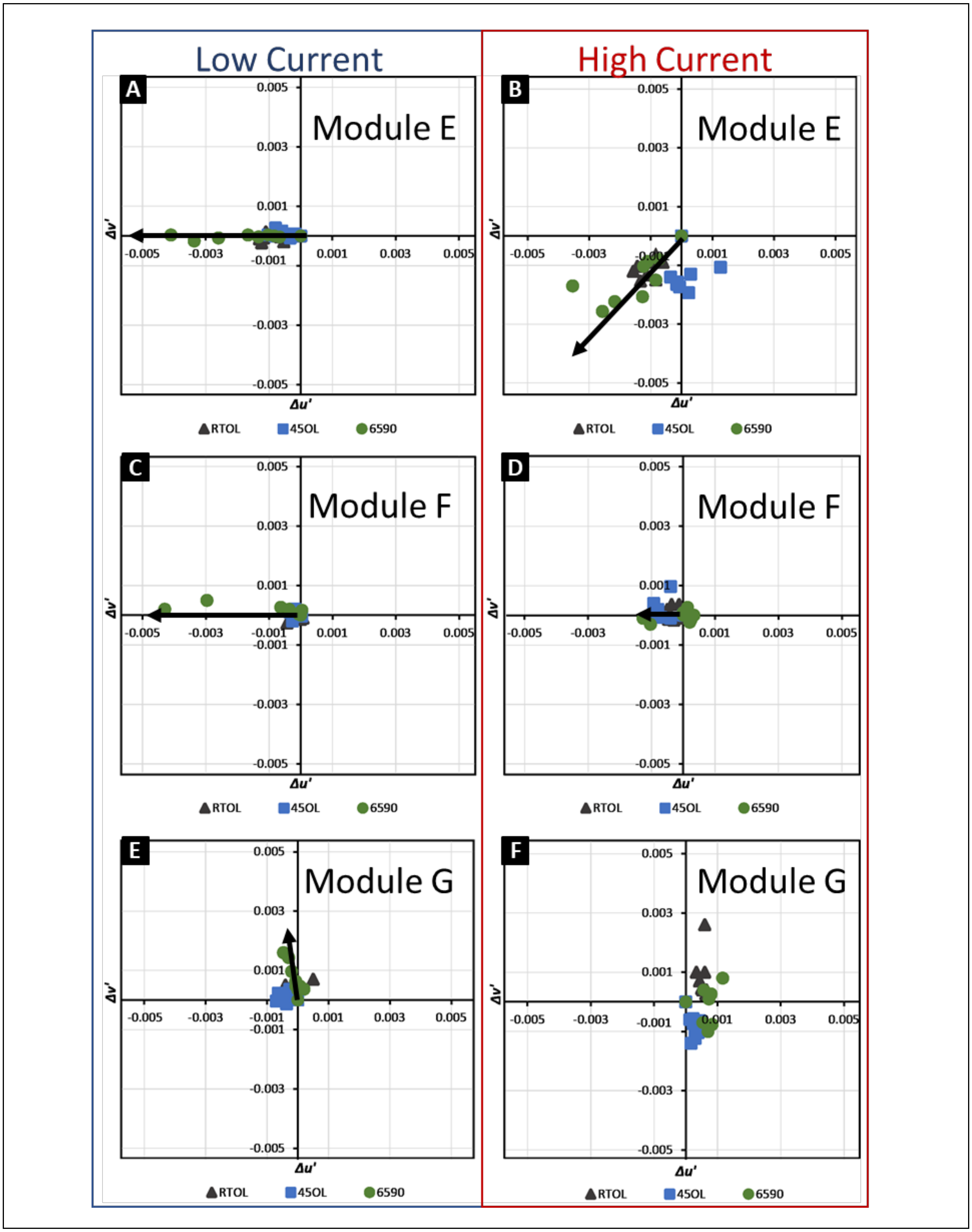

Figure 3-18. Chromaticity diagram for (A) Module E at low current, (B) Module E at high current, (C) Module F at low current, (D) Module F at high current, (E) Module G at low current, and (F) Module G at high current.

The operational Module G DUTs exhibited different chromaticity shift behavior than their low-CCT counterparts. At low current, the chromaticity shifted slowly in the yellow direction (i.e., chromaticity changed in the $+\Delta v'$ axis with minimal change in the $\Delta u'$ axis) as shown in **Figure 3-18E**. The magnitude of these shifts was small ($\Delta u'v' < 0.0017$) and the shifts were not accompanied by large changes in phosphor peak position. At high current, the magnitude of the chromaticity shifts remained small ($\Delta u'v' < 0.0015$) at all time points during test as shown in **Figure 3-18F**. The chromaticity shift for the Module G DUTs at high current appeared to be random, and a CSM was unable to be determined.

3.2.3 Electrical Analysis of LED Modules

In general, the operational DUTs of Module E – Module G experienced minimal changes in power consumption for the duration of the testing period (7,000 hrs of RTOL and 45OL; 6,000 hrs of 6590). The largest increase in power consumption was observed for the Module F DUTs at high current setting, but this increase was still less than 0.2 W, which resulted in an increase in power consumption of less than 4%. Though the operational DUTs maintained stable power consumption with aging, 4 of the 27 DUTs (there were 9 DUTs for each LED module [E – F] at three test conditions [RTOL, 45OL, 6590]) failed parametrically or abruptly by the end of the test. In three of these DUTs, power consumption changed drastically. The failure description, AST conditions, and time to failure for each LED module are summarized in **Table 3-8**.

Table 3-8. LED Module Failure Descriptions.

Module ID	DUT	AST	Failure Type – Current Level	Time to Failure (hr)
E	487	45OL	Parametric (chromaticity shift) – High Current	6,000
F	582	6590	Parametric (chromaticity shift) – Low Current	6,000
G	589	RTOL	Parametric (chromaticity shift) – Low Current Parametric (chromaticity shift) – High Current	5,000 4,000
G	591	RTOL	Abrupt – Low Current Parametric (LFM < 0.70, chromaticity shift) – High Current	6,000 6,000

The parametric chromaticity shift failures for the lower CCT LED modules (Module E and Module F) only occurred at one current setting. For both failures, incorrect LEDs were illuminated at the failed current setting. For Module E DUT 487, a strip of LEDs on the left side of the COB beneath the phosphor encapsulation stopped emitting light at high current setting, and this appeared to concentrate current onto the right side of the COB. This caused a chromaticity shift failure for DUT 487 in the blue direction ($-\Delta u$ and $-\Delta v'$) with magnitude $\Delta u'v' = 0.0185$ as shown in **Figure 3-19**. The chromaticity shift likely resulted from the concentration of current on the right side of the COB, leading to more blue LED emission on the right side than initially designed. It is likely that the concentration of phosphor around these LEDs was insufficient to fully convert the additional blue emissions, resulting in more blue emissions that caused the observed blue shift. The failure caused an increase in the voltage needed to power the DUT (18.55 V to 19.89 V) and LFM increased by 10%. The parametric chromaticity shift failure experienced by Module F (DUT 582) proceeded in the green direction ($-\Delta u$) with magnitude $\Delta u'v' = 0.0072$ only at low current settings. At the low current setting, only the two lower CCT CSPs should emit light for the Module F DUTs as shown in **Appendix B**. However, DUT 582 had a third CSP (higher CCT) illuminated at low power after failure occurred. In addition, DUT 582 experienced very little change in power consumption (less than 0.01 W) after failure. Therefore, the chromaticity shift was caused by less power supplied to the lower CCT CSPs (loss of green emissions). This incorrect regulation of current to the CSPs could be due to logic failure but more investigation is needed to determine an exact cause.

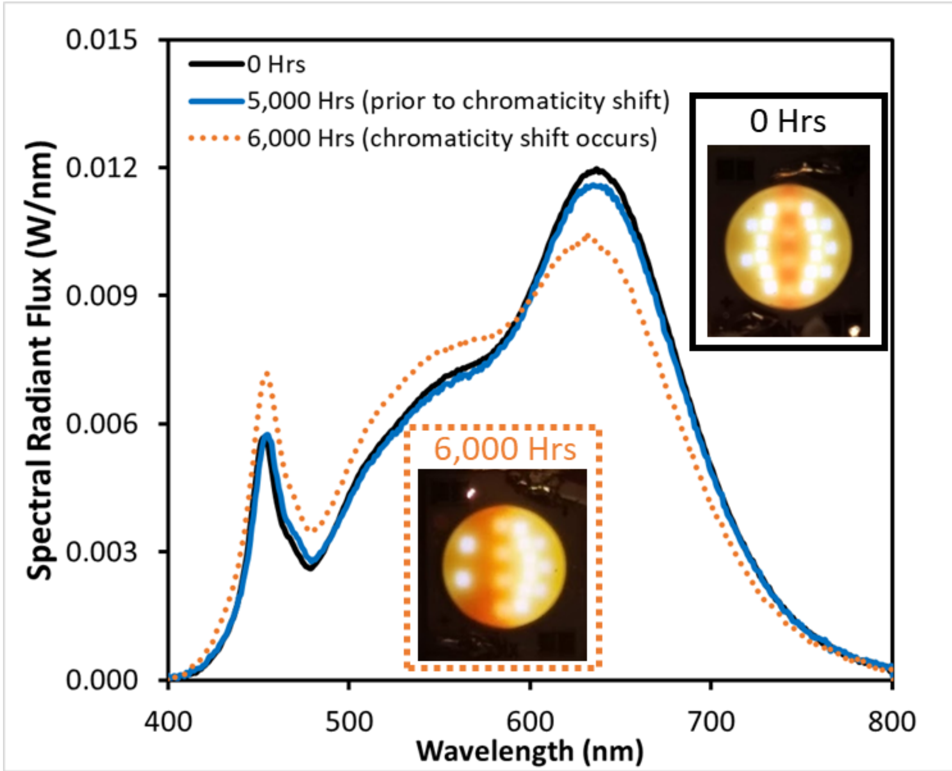

Figure 3-19. SPD of Module E DUT 487 at 6,000 hrs shows increased radiant flux in the blue-green region (450 nm – 550 nm) relative to the starting SPD (0 hrs) and SPD taken at 5,000 hrs just prior to parametric failure. Pictures of the DUT show loss of light emission from LEDs on the left side of the COB at 6,000 hrs.

Two DUTs failed for the higher CCT LED module (Module G). Both were operated at RTOL and failed at all current levels by the end of testing. At all current settings, only the higher CCT CSPs of DUT 589 emitted light by the end of testing. This led to large increases in radiant flux in the blue region ($\Delta u'v' \geq 0.0385$) as shown in **Figure 3-20A**. The voltage necessary to operate DUT 589 also increased (from 14.77 V to 17.90 V at low current and from 18.32 V to 20.90 V at high current) and LFM increased to 1.80 at the low current setting. The exact cause of failure for DUT 589 is unknown, but the improper current regulation suggests a control IC failure. While DUT 589 produced excessive light in the blue region, DUT 591 output no light at the low current setting and low light (LFM = 0.18) at the high current setting. Moreover, the light emission at high current was only produced by one CSP (the lower CCT LED primary), which resulted in a much warmer CCT than initially programmed (2,591 K vs. 3,974 K). The cause of failure for DUT 589 was likely a manufacturing flaw: solder migration shorted two pins of the control IC together as shown in **Figure 3-20B**. Once the pins were shorted, the control IC was no longer able to properly regulate current to the CSPs.

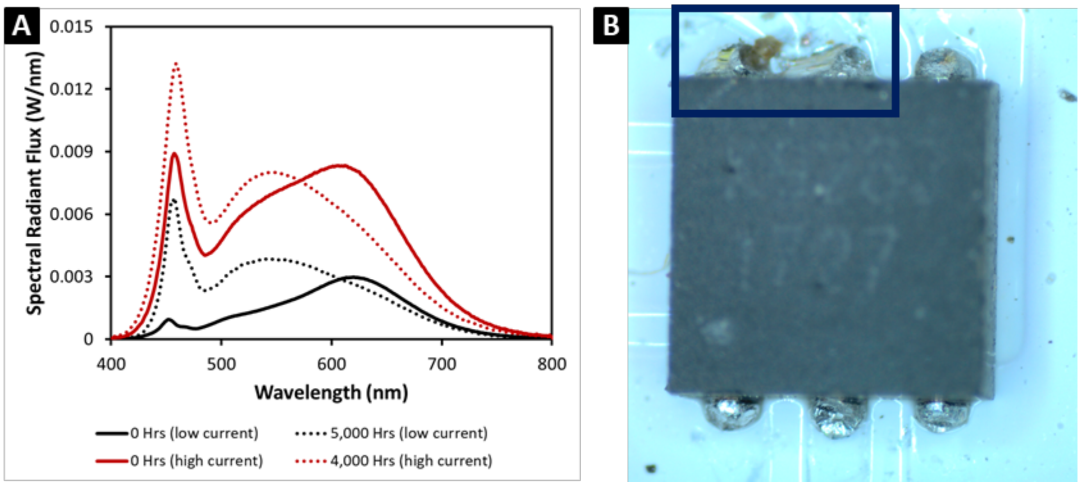

Figure 3-20. (A) SPDs of DUT 589 post-failure (dashed lines) showed increases in blue emissions compared to the SPDs taken at 0 hrs (solid lines) at both low (black) and high (red) current settings. (B) The blue box shows an electrical short created between two pins of DUT 591's control IC.

4 Conclusions

The components, electrical complexity, and limited physical space needed to achieve warm-dimming behavior presents new challenges to the reliability and long-term device performance of D2W products. The data in this report lead to the conclusion that D2W products operated at mild conditions (e.g., RTOL, 45OL) have reasonable projected lifetimes (projected lifetime was limited only by the duration of test) and minimal chromaticity shift. With additional stressors (e.g., heat, humidity), performance of the DUTs was reduced, with DUTs with smaller form factors (e.g., candelabras vs. A-style lamps) being more affected by the stressors. Further, the lower CCT LED primaries were more susceptible to these stressors (evidenced by larger chromaticity shifts and radiant flux loss) than higher CCT LED primaries, likely due to greater amounts of phosphor oxidation. Lower CCT LED primaries (CCT of 1,800 K – 2,200 K) are needed to achieve the familiar warm white spectrum of an incandescent lamp upon dimming, and the results of these data suggest that future research should address these instabilities. In addition, premature parametric failure occurred in 5 DUTs (out of 63 total DUTs) as a result of electrical or logic failure at the low stress conditions of RTOL and 45OL (i.e., prior to expected wear-out failure times). These failures indicate that attention should be focused toward the manufacturing processes around the logic circuits and components' reliability in these circuits. Understanding the impacts of the electrical architectures, form factors, LED packages, and secondary optics is critical to understanding the long-term reliability of D2W devices, and the information and data about these topics presented in this report are critical to the development of D2W products with long lifetimes and high reliabilities.

References

1. Next Generation Lighting Industry Alliance and LED Systems Reliability Consortium. (2019, July). *Dim-to-Warm LED Lighting: Initial Benchmarks*. Available at https://www.nglia.org/documents/LSRC_Dim-to-Warm_Paper_final_073019r.pdf.

2. Buccitelli, N., Elliott, C., Schober, S., Yamada, M. (2017, November). *2015 U.S. Lighting Market Characterization*. Washington, DC: U.S. Department of Energy. Available at https://www.energy.gov/sites/prod/files/2017/12/f46/lmc2015_nov17.pdf.

3. Davis, R. G. & Wilkerson, A. (2017, September). *Tuning the Light in Classrooms: Evaluating Trial LED Lighting Systems in Three Classrooms at the Carrollton-Farmers Branch Independent School District in Carrollton, TX*. Washington, DC: U.S. Department of Energy. Available at https://www.energy.gov/sites/prod/files/2017/10/f37/2017_gateway_tuning-classroom_0.pdf.

4. Wilkerson, A., Davis, R.G., & Clark, E. (2017, August). *Tuning Hospital Lighting: Evaluating Tunable LED Lighting at the Swedish Hospital Behavioral Health Unit in Seattle*. Washington, DC: U.S. Department of Energy. Available at https://www.energy.gov/sites/prod/files/2017/08/f36/2017_gateway_swedish-tuning-led_0.pdf.

5. Stober, K., Lee, K.,. Yamada, M., & Pattison, M. (2017, December). *Energy Savings Potential of SSL in Horticultural Applications*. Washington, DC: U.S. Department of Energy. Available at https://www.energy.gov/sites/prod/files/2017/12/f46/ssl_horticulture_dec2017.pdf.

6. ANSI (American National Standards Institute) and IES (Illuminating Engineering Society) (2019). *ANSI/IES LM-79-19: Approved Method: Optical and Electrical Measurements of Solid-State Lighting Products*. New York, NY: IES.

7. IES (Illuminating Engineering Society). (2014). *IES TM-28-14: Projecting Long-Term Luminous Flux Maintenance of LED Lamps and Luminaires*. New York, NY: IES.

8. Yeh, C.-W., Chen, W.-T., Liu, R.-S., Hu, S.-F., Sheu, H.-S., Chen, J.-M., & Hintzen, H. T. (2012). Origin of thermal degradation of Sr(2-x)Si5N8:Eu(x) phosphors in air for light-emitting diodes. *Journal of the American Chemical Society, 134*(34), 14108–14117.

9. Next Generation Lighting Industry Alliance and the LED Systems Reliability Consortium. (2017, April). *LED Luminaire Lifetime: Impact of Color Shift*. Available at https://www.nglia.org/pdfs/lsrc_colorshift_apr2017r.pdf.

10. Davis, J. L., Mills, K., Yaga, R., Johnson, C., Hansen, M., & Royer, M. (2018). Chromaticity maintenance in LED devices. In *Solid State Lighting Reliability Part 2: Components to Systems*. Van Driel, W., Fan, X., & Zhang, G. (eds.). New York, NY: Springer.

11. Dutta, A. 2019. *SSL lamps and luminaires: Technology perspective*. Presentation at the 2019 DOE SSL R&E Workshop. Dallas, TX. Available at https://www.energy.gov/sites/prod/files/2019/02/f59/dutta-luminaires_ssl-rd2019.pdf.

12. Davis, J. L. & Rountree, K. (2019, February). Accelerated Stress Testing Results on Single-Channel and Multi-Channel Drivers: Final Report. Washington, DC: U.S. Department of Energy. Available at https://www.energy.gov/sites/prod/files/2019/08/f65/ssl_rti_single-multi-channel_driver_final_0.pdf.

13. NEMA (National Electrical Manufacturers Association). (2017). NEMA 77-2017 Standard for Temporal Light Artifacts: Test Methods and Guidance for Acceptance Criteria.

14. IEEE (Institute of Electrical and Electronics Engineers). (2015). IEEE Std 1789-2015: IEEE Recommended Practices for Modulating Current in High-Brightness LEDs for Mitigating Health Risks to Viewers.

15. Mehr, Y., Bahrami, A., van Driel, W. D., Fan, X. J., Davis, J. L., & Zhang, G.Q. (2019, January). Degradation of optical materials in solid-state lighting systems. *International Materials Reviews*, 1-27. https://doi.org/10.1080/09506608.2019.1565716.

Appendix A

A characteristics summary of Lamp A – Lamp D is provided here from our previous report [1]. Each figure contains the following: 1) images to show which LEDs (LED filaments) emit light at different power levels (listed as a percentage value of full power), 2) a table of LED lamp flux, efficacy, chromaticity point, color quality metrics, and CCT values at three input power levels, and 3) the normalized SPD for different input power levels are shown in the lower right graph. Note that the input power listed reflects the entire system including the Z-Wave Dimmer and DUT.

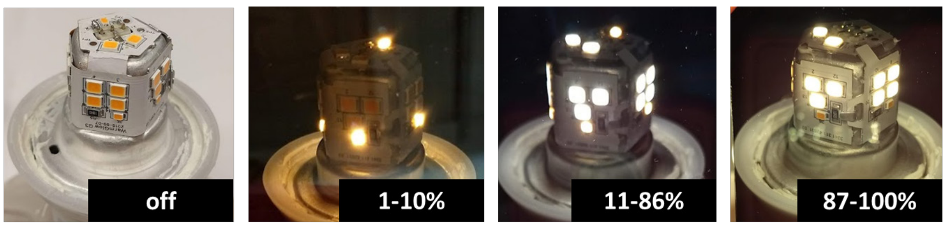

	10%	50%	100%
Lumens	46.8 lm	507 lm	815 lm
System Input Power	1.6 W	6.5 W	10.0 W
Luminous Efficacy	29.2 lm/W	95.0 lm/W	81.5 lm/W
u′	0.2918	0.2601	0.2595
v′	0.5354	0.5278	0.5282
R_f	84	85	85
R_g	98	95	94
CCT	2175 K	2745 K	2758 K
Centroid λ	610 nm	589 nm	589 nm

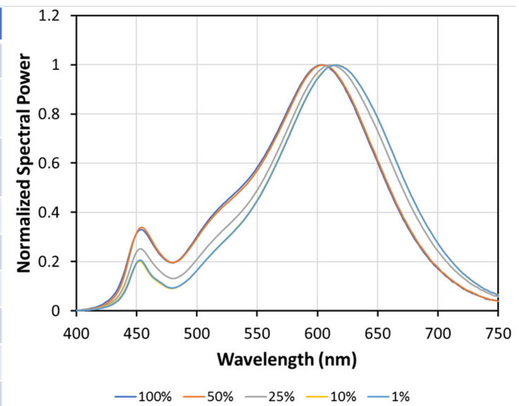

Figure A-1. Characteristics of Lamp A.

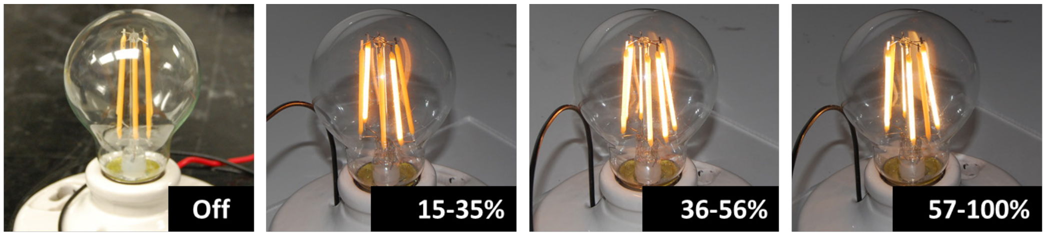

	25%	50%	100%
Lumens	88.1 lm	513 lm	819 lm
System Input Power	1.9 W	5.4 W	8.1 W
Luminous Efficacy	46.4 lm/W	95.0 lm/W	101.1 lm/W
u′	0.2951	0.2694	0.2619
v′	0.5367	0.5283	0.5266
R_f	84	85	83
R_g	94	93	92
CCT	2129 K	2558 K	2713 K
Centroid λ	608 nm	593 nm	588 nm

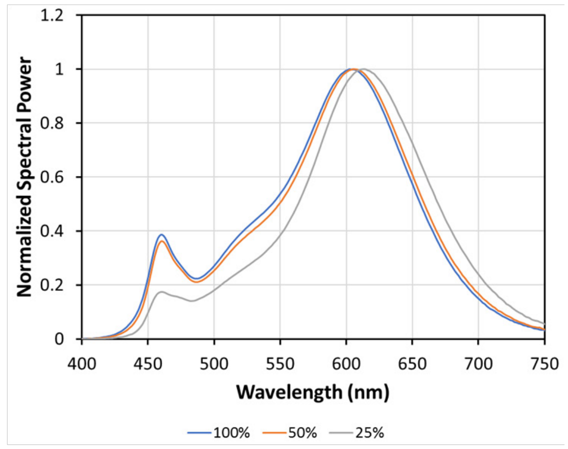

Figure A-2. Characteristics of Lamp B.

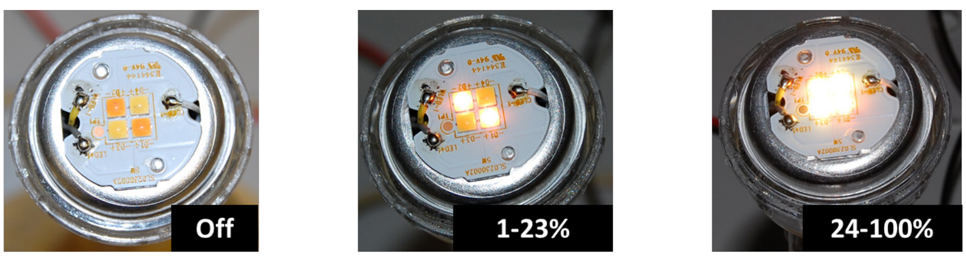

	10%	50%	100%
Lumens	22.0 lm	189 lm	329 lm
System Input Power	1.1 W	3.7 W	5.3 W
Luminous Efficacy	20 lm/W	51.1 lm/W	62.1 lm/W
u′	0.3272	0.2852	0.2658
v′	0.5413	0.5322	0.5274
R_f	87	90	91
R_g	91	99	98
CCT	1758 K	2279 K	2631 K
Centroid λ	623 nm	606 nm	597 nm

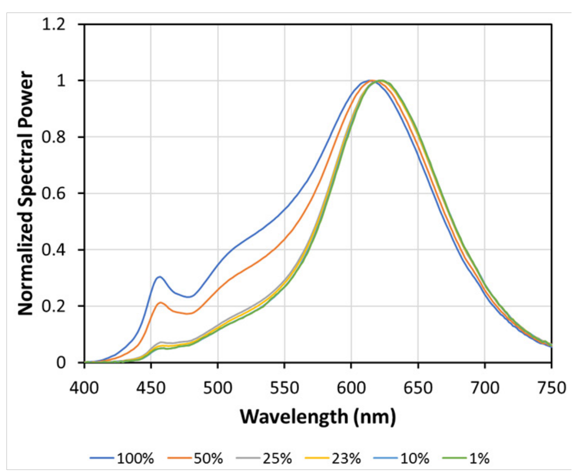

Figure A-3. Characteristics of Lamp C.

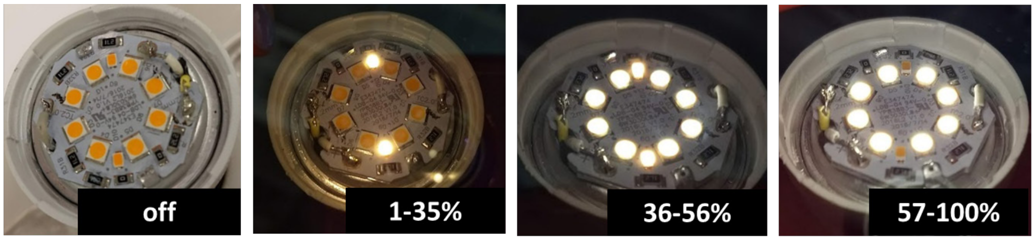

	10%	50%	100%
Lumens	8.22 lm	227 lm	500 lm
System Input Power	1.0 W	4.0 W	6.0 W
Luminous Efficacy	8.22 lm/W	56.8 lm/W*	83.3 lm/W
u′	0.2950	0.2652	0.2628
v′	0.5323	0.5258	0.5256
R_f	84	85	84
R_g	97	96	96
CCT	2134 K	2649 K	2698 K
Centroid λ	610 nm	591 nm	591 nm

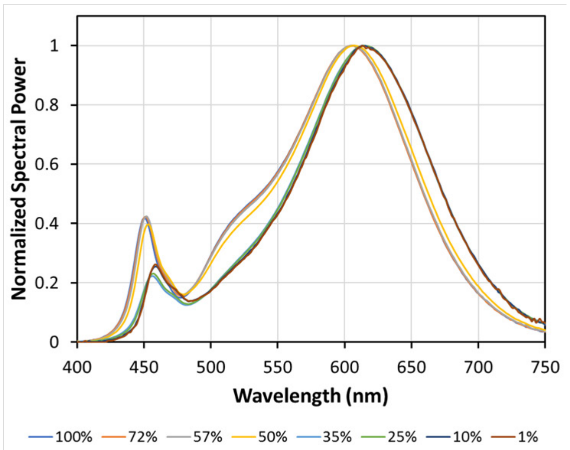

Figure A-4. Characteristics of Lamp D.

Appendix B

Characteristic summaries of LED modules (Module E, Module F, and Module G) are updated here from our previous report [1]. Each figure contains the following: 1) images to show which LEDs or CSPs emit light at different drive currents, 2) a table of flux, efficacy, chromaticity point, color quality metrics, and CCT values at the three operational input dc levels, and 3) the normalized SPD for different input dc levels are shown in the lower right graph.

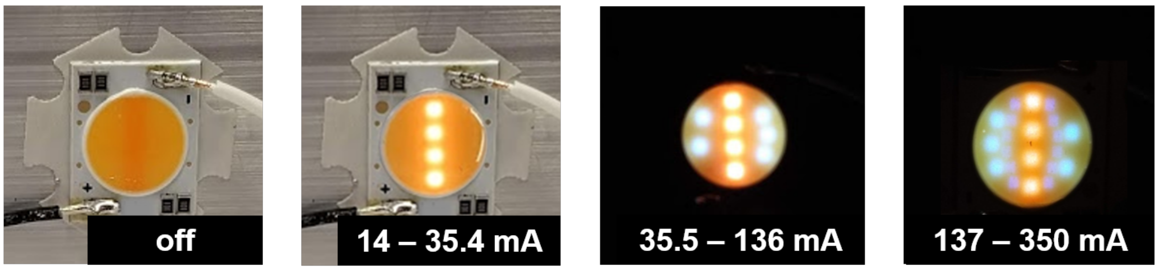

	32 mA	130 mA	350 mA
Lumens	32 lm	170 lm	583 lm
Voltage	12.40 V	15.73 V	17.84 V
Luminous Efficacy	80.9 lm/W	83.1 lm/W	93.4 lm/W
u′	0.3289	0.2692	0.2506
v′	0.5449	0.5249	0.5187
R_f	93	95	95
R_g	100	104	102
CCT	1814 K	2501 K	3014 K
Centroid λ	634.9 nm	615.5 nm	602.7 nm

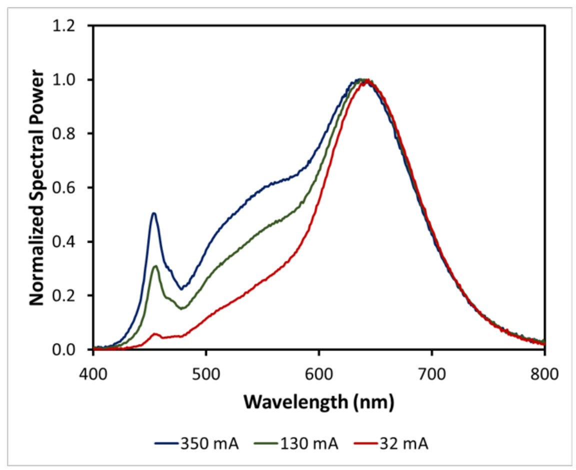

Figure B- 1. Characteristics of Module E.

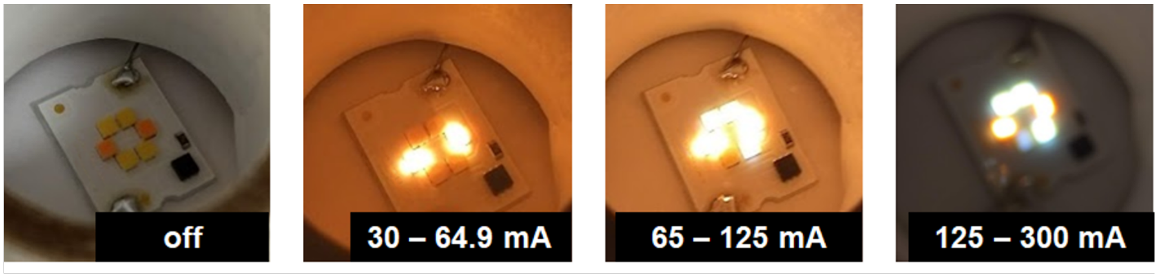

	60 mA	120 mA	300 mA
Lumens	61 lm	183 lm	538 lm
Voltage	14.26 V	16.51 V	18.91 V
Luminous Efficacy	71.7 lm/W	92.3 lm/W	94.9 lm/W
u′	0.3289	0.2692	0.2506
v′	0.5449	0.5249	0.5187
R_f	82	91	90
R_g	78	100	98
CCT	1741 K	2572 K	3015 K
Centroid λ	634.1 nm	605.1 nm	592.1 nm

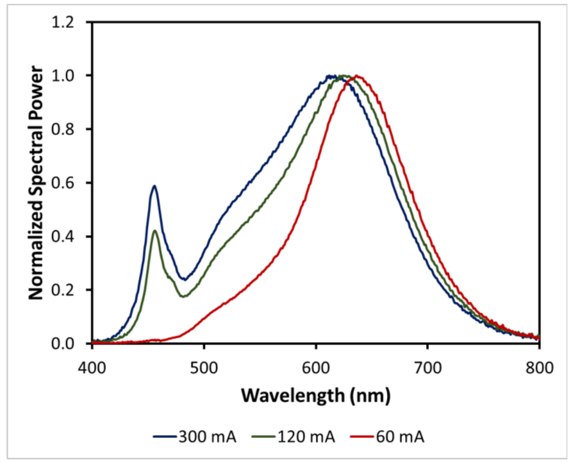

Figure B- 2. Characteristics of Module F.

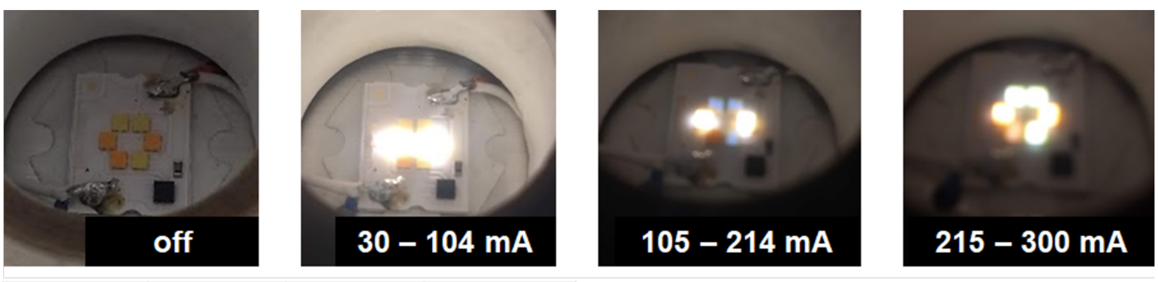

	100 mA	213 mA	300 mA
Lumens	141 lm	373 lm	535 lm
Voltage	14.94 V	17.44 V	18.47 V
Luminous Efficacy	94.3 lm/W	100.4 lm/W	96.6 lm/W
u′	0.2639	0.2261	0.2246
v′	0.5294	0.5049	0.5033
R_f	91	88	88
R_g	97	95	95
CCT	2661 K	3906 K	3986 K
Centroid λ	601 nm	577 nm	575.6 nm

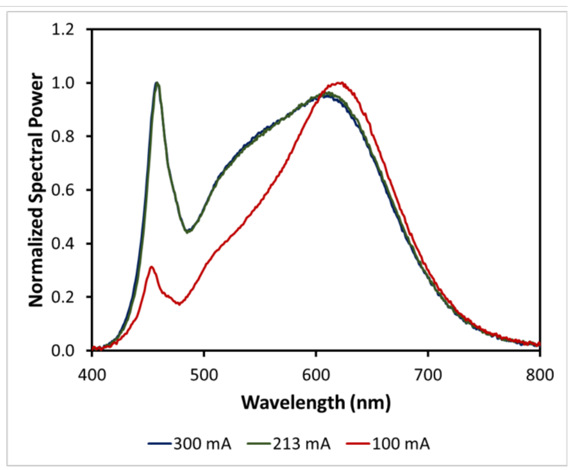

Figure B- 3. Characteristics of Module G.

(This page intentionally left blank)

U.S. DEPARTMENT OF
ENERGY

Office of
ENERGY EFFICIENCY &
RENEWABLE ENERGY

For more information, visit:
energy.gov/eere/ssl

DOE/EERE-2047 ▪ January 2020